



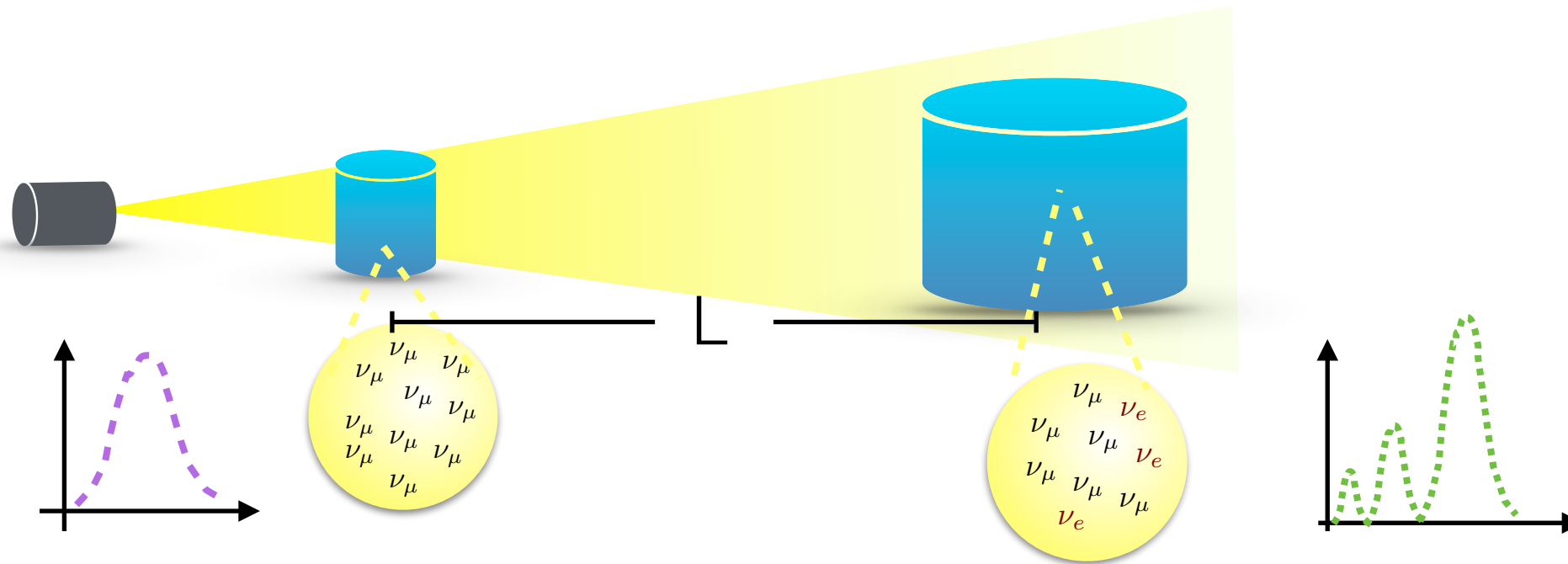
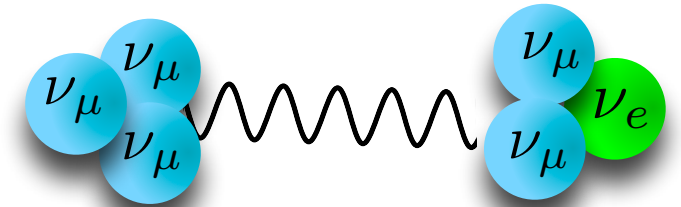
# Neutrino cross section updates

Noemi Rocco

Nuphys 2023: Prospects in Neutrino Physics  
King's College London — December 18 - 20, 2023

# Addressing Neutrino-Oscillation Physics

$$P_{\nu_\mu \rightarrow \nu_e}(E, L) \sim \sin^2 2\theta \sin^2 \left( \frac{\Delta m^2 L}{4E} \right) \rightarrow \Phi_e(E, L) / \Phi_\mu(E, 0)$$



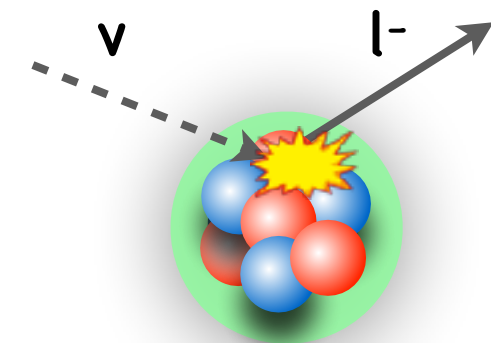
Detectors measure the **neutrino interaction rate**:

$$N_e(E_{\text{rec}}, L) \propto \sum_i \Phi_e(E, L) \sigma_i(E) f_{\sigma_i}(E, E_{\text{rec}}) dE$$

Reconstructed  
ν energy

Cross Section

Smearing  
matrix



A precise determination of  $\sigma(E)$  is crucial to extract ν oscillation parameters



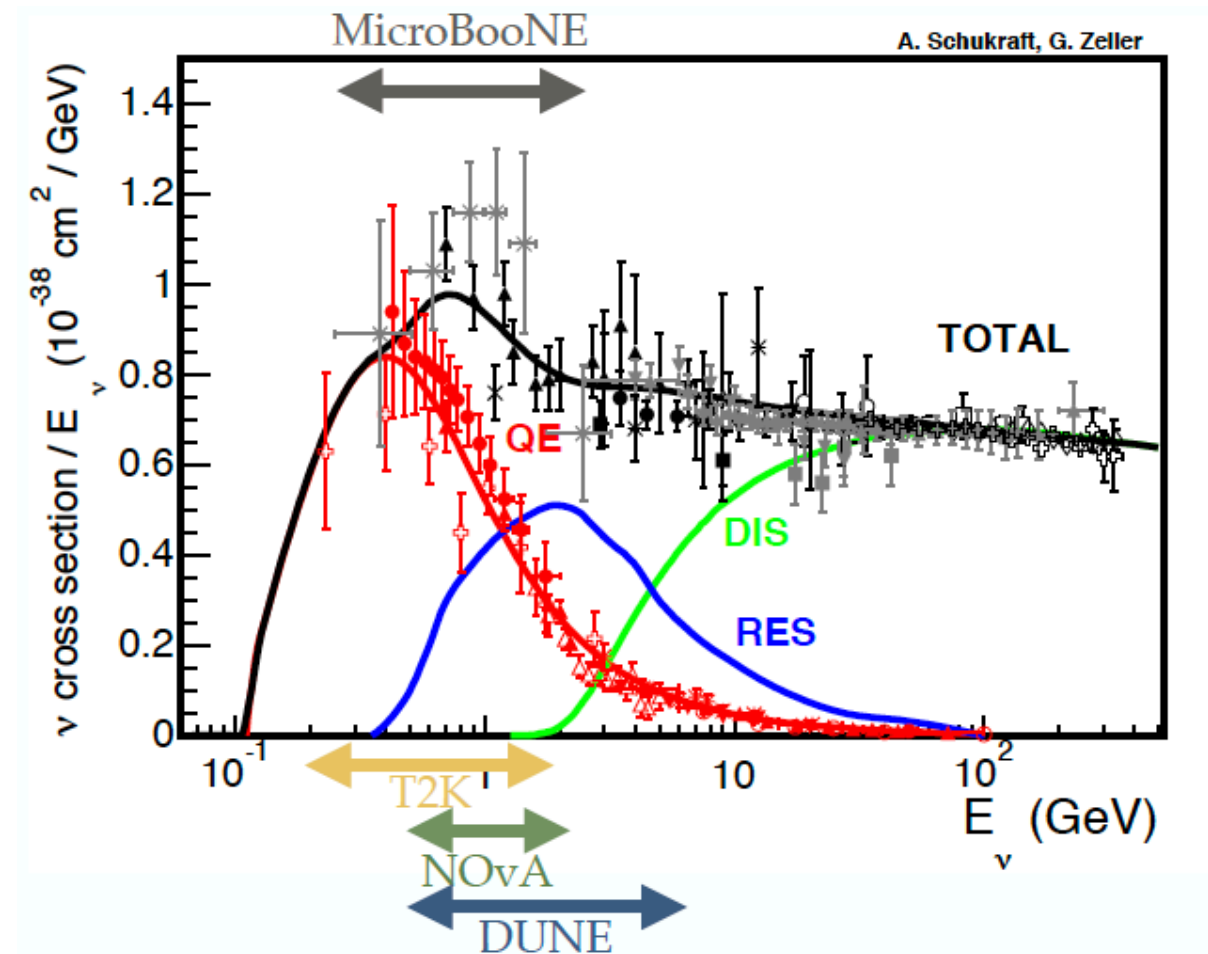
# Inputs for the nuclear model

**Unprecedented accuracy** in the determination of **neutrino-argon cross section** is required to achieve design sensitivity to CP violation at DUNE

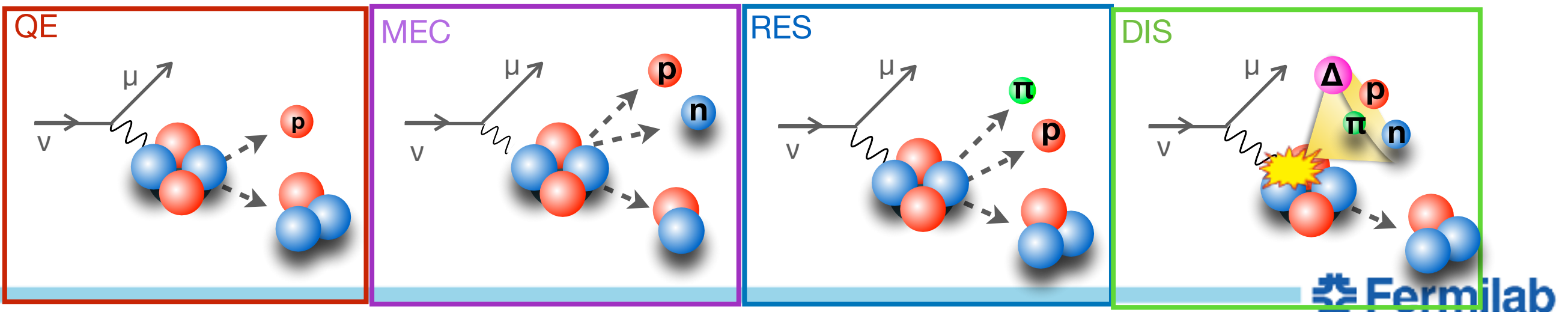
More than 60% of the interactions at DUNE are non-quasielastic

For SBN and T2K the dominant reaction mechanisms are quasi-elastic scattering; the contribution of  $\pi$ -production channels is  $\sim 25\%$

SBND will provide the world's highest statistics cross section measurements in LAr: 2 million events for  $\nu_\mu$  per year for the next 3 years




Theoretical tools for neutrino scattering,  
Contribution to: 2022 Snowmass Summer Study

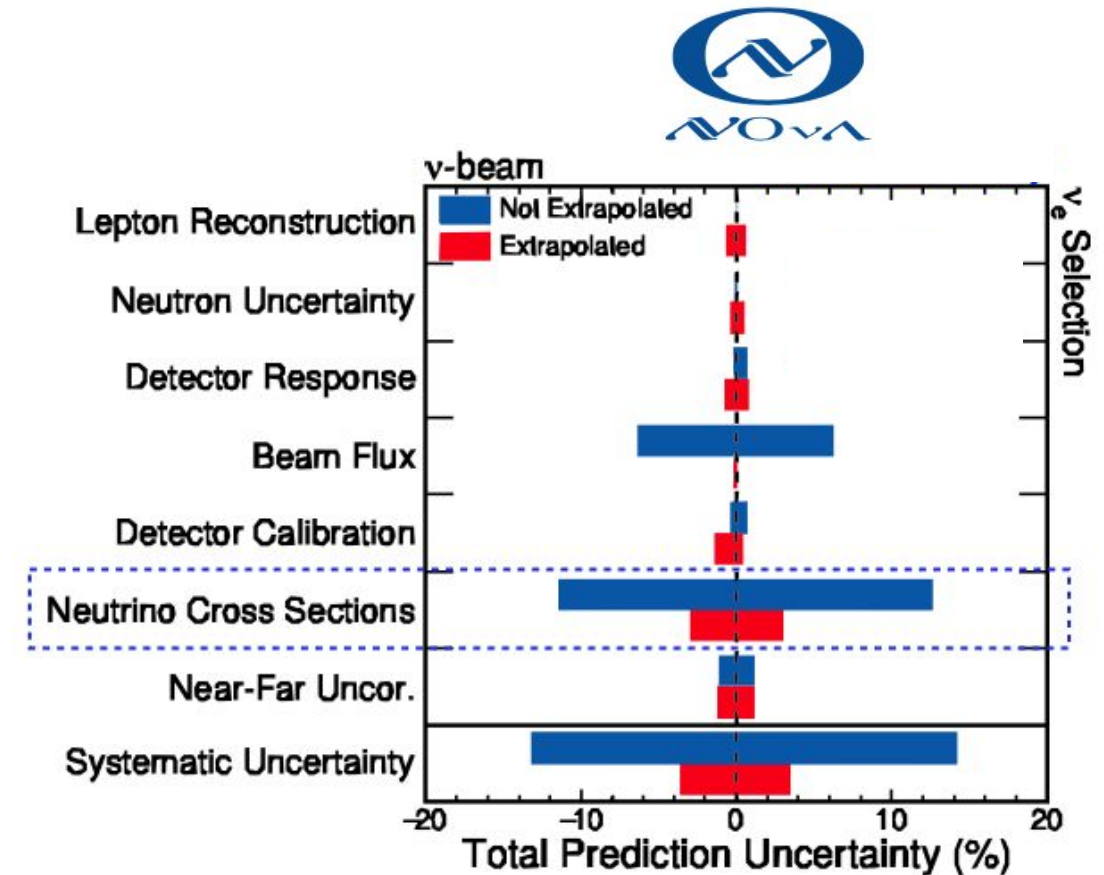


# Neutrino-nucleus cross section systematics

Current oscillation experiments report **large systematic uncertainties** associated with neutrino-nucleus interaction models.



Error source	$\nu_e$ FHC	$\bar{\nu}_e$ RHC	$\nu_e / \bar{\nu}_e$ FHC/RHC
Flux and (ND unconstrained) cross section (ND constrained)	15.1	12.2	1.2
SK detector	2.8	3.8	1.5
SK FSI + SI + PN	3.0	2.3	1.6
Nucleon removal energy	7.1	3.7	3.6
$\sigma(\nu_e)/\sigma(\bar{\nu}_e)$	2.6	1.5	3.0
NC1 $\gamma$	1.1	2.6	1.5
NC other	0.2	0.3	0.2
$\sin^2 \theta_{23}$ and $\Delta m_{21}^2$	0.5	0.3	2.0
$\sin^2 \theta_{13}$ PDG2018	2.6	2.4	1.1
All systematics	8.8	7.1	6.0

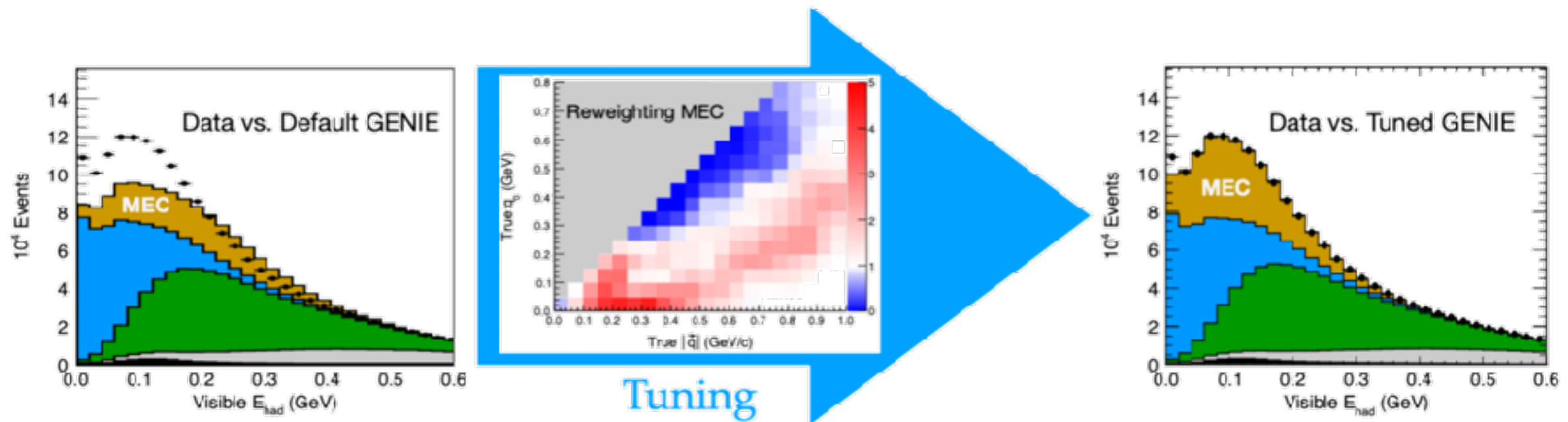


T2K, Phys. Rev. D 103, 112008 (2021)



# Tuning

Discrepancies between generators and data often corrected by tuning an empirical model of the least well known mechanism: MEC (“meson exchange”/two-body currents)



Coyle, Li, and Machado, JHEP 12, 166 (2022)

Mis-modeling can distort signals of new physics, **biasing** measurement of **new physics parameters**

Studies on the impact of different neutrino interactions and nuclear models on determining neutrino oscillation parameters are critical. These enable us to assess the level of precision we aim at.

Coloma, et al, Phys.Rev.D 89 (2014) 7, 073015

# Theory of lepton-nucleus scattering

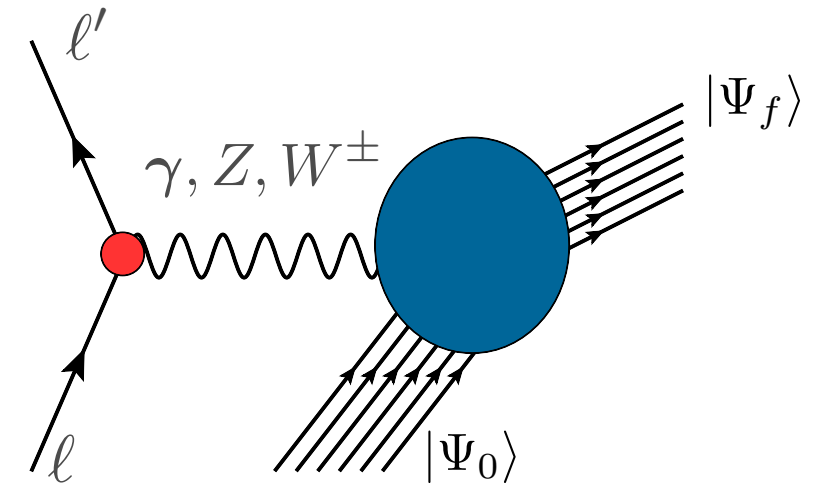
- The cross section of the process in which a lepton scatters off a nucleus is given by

$$d\sigma \propto L^{\alpha\beta} R_{\alpha\beta}$$

Leptonic Tensor: can include new physics models

Hadronic Tensor: nuclear response function

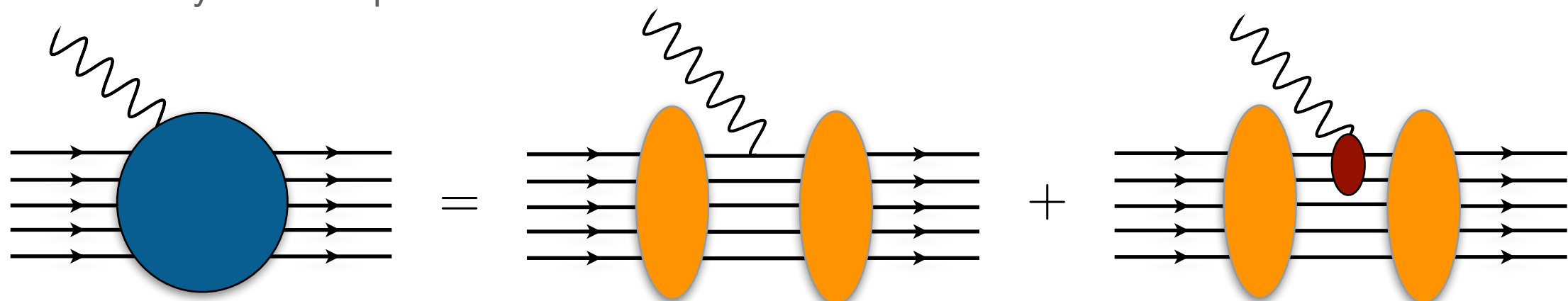
$$R_{\alpha\beta}(\omega, \mathbf{q}) = \sum_f \langle 0 | J_\alpha^\dagger(\mathbf{q}) | f \rangle \langle f | J_\beta(\mathbf{q}) | 0 \rangle \delta(\omega - E_f + E_0)$$



The initial and final wave functions describe many-body states:

$$|0\rangle = |\Psi_0^A\rangle, |f\rangle = |\Psi_f^A\rangle, |\psi_p^N, \Psi_f^{A-1}\rangle, |\psi_k^\pi, \psi_p^N, \Psi_f^{A-1}\rangle \dots$$

One and two-body current operators

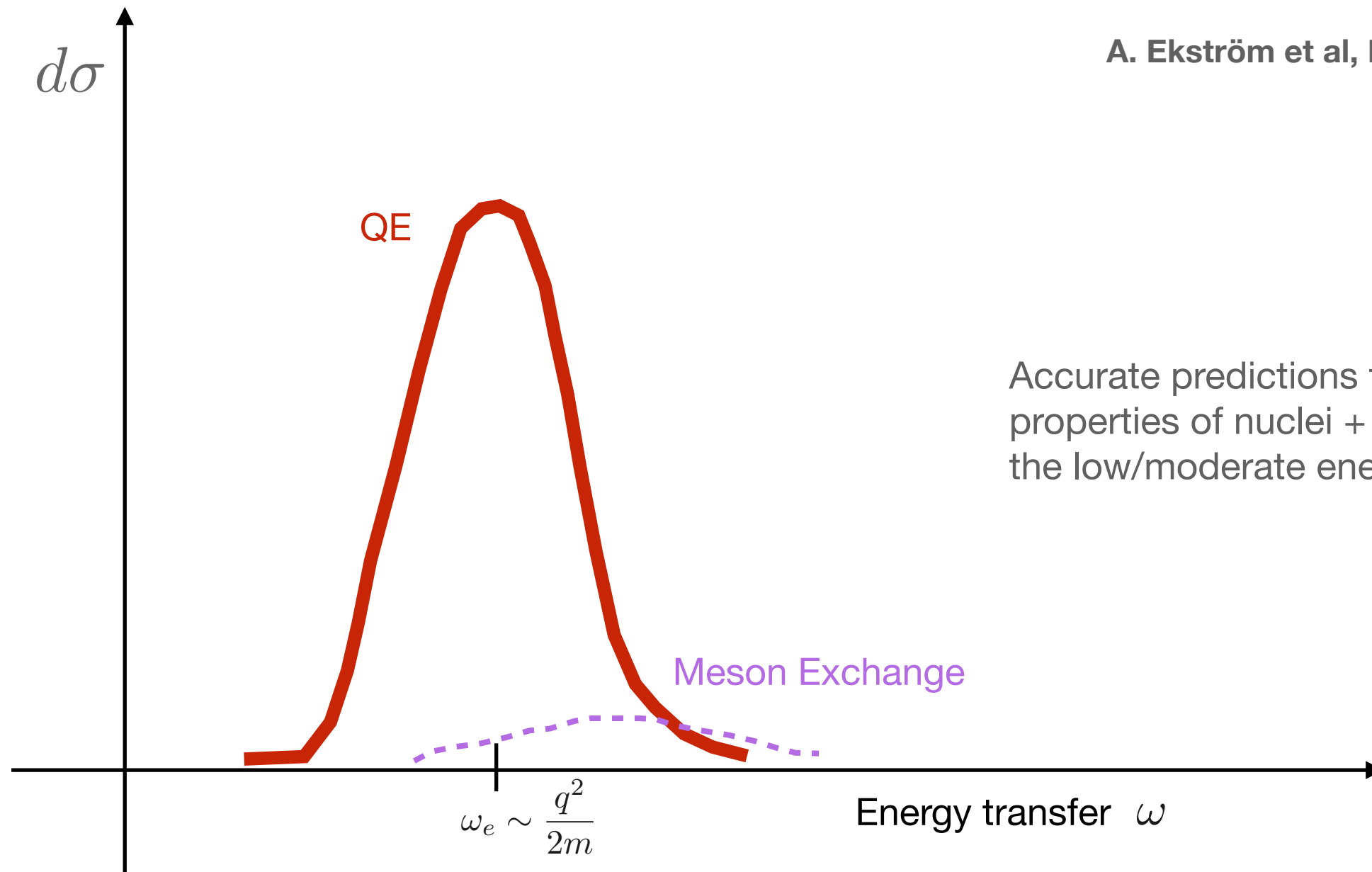




# Ab initio Methods

Ab-initio methods (CC, IMSRG, SCGF, QMC, etc) are systematically improvable many-body approaches.

A. Ekström et al, *Front. Phys.*11 (2023) 29094

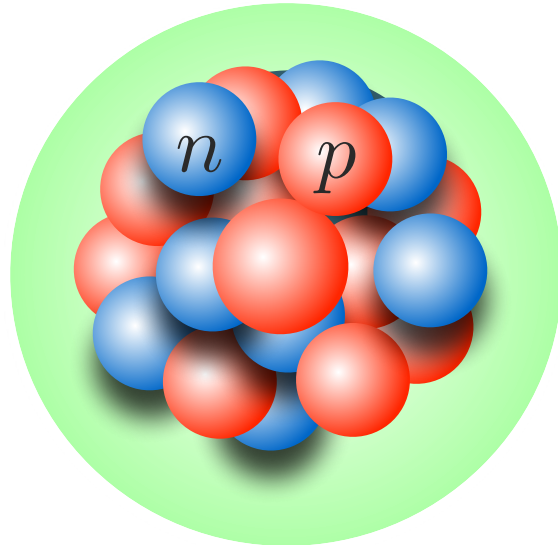


Accurate predictions for ground state properties of nuclei + response functions in the low/moderate energy region

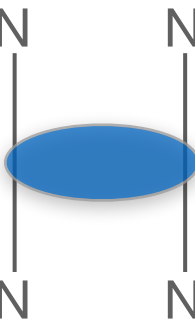
# Hamiltonian & Current operators

At low energy, the effective degrees of freedom are pions and nucleons:

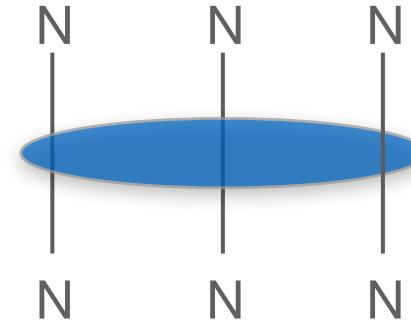
$$H = \sum_i \frac{\mathbf{p}_i^2}{2m} + \sum_{i < j} v_{ij} + \sum_{i < j < k} V_{ijk} + \dots$$



**1-body**



**2-body**



**3-body**

Different strategies to construct two- and three-body interactions

- ❖ Chiral Effective Field Theory interactions
- ❖ Phenomenological potentials



# Hamiltonian & Current operators

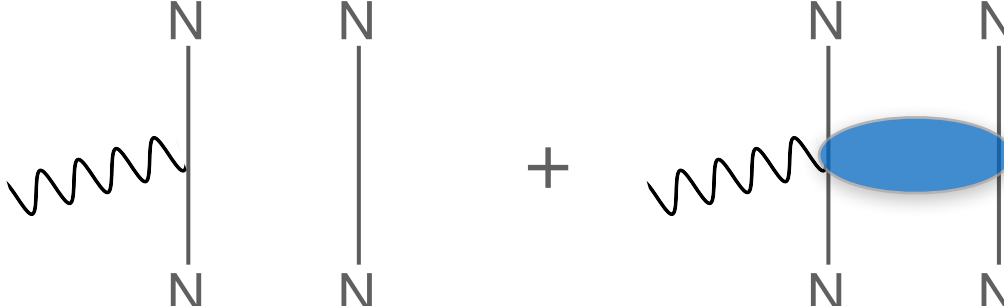
The current operator describes how the external probe interacts with nucleon, nucleons pairs, create new particles ...

The structure of the current operator is constrained by the Hamiltonian through the continuity equation

$$\nabla \cdot \mathbf{J}_{\text{EM}} + i[H, J_{\text{EM}}^0] = 0$$

$$[v_{ij}, j_i^0] \neq 0$$

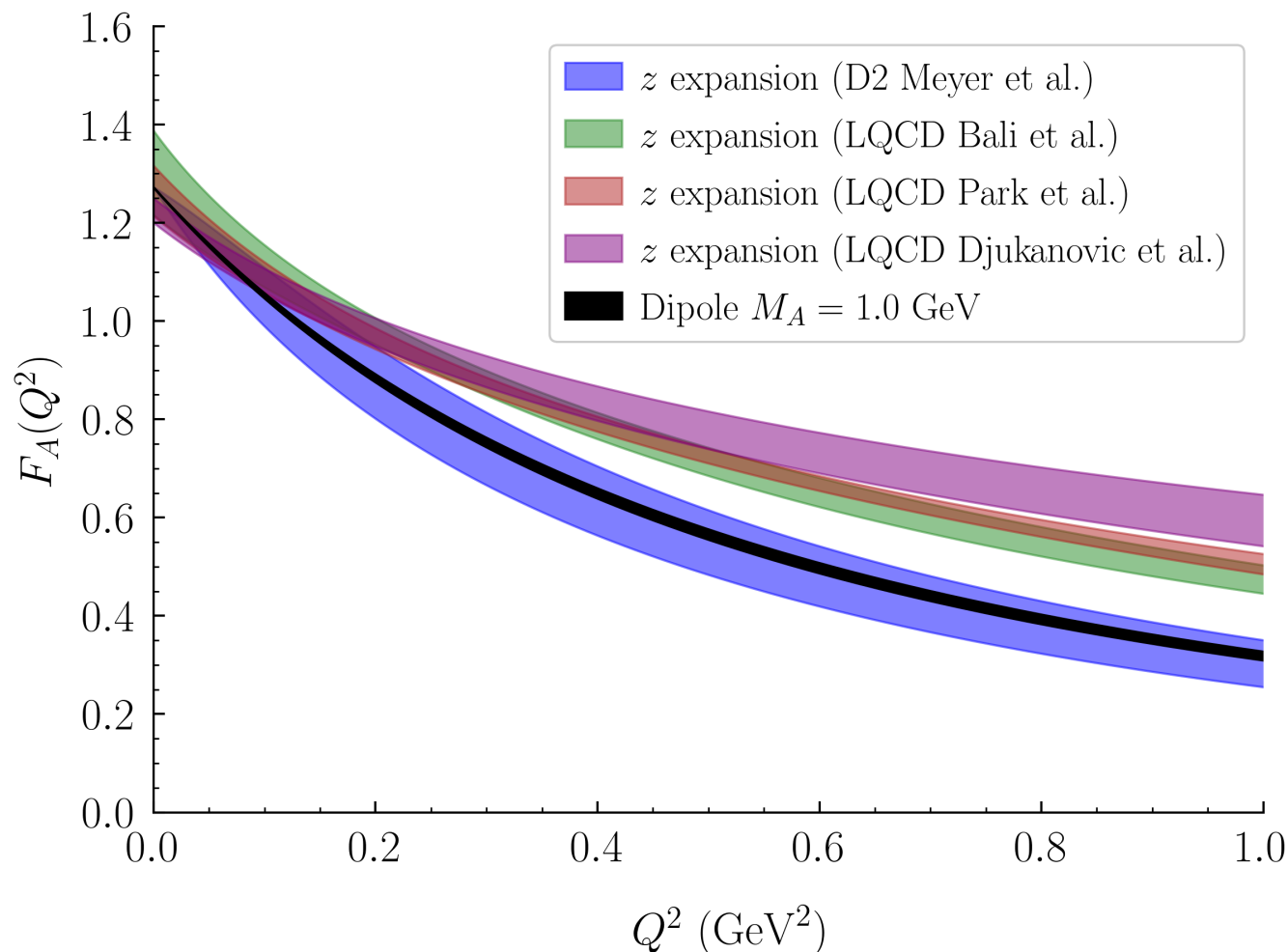
The Hamiltonian structure implies that the current operator includes one and two-body contributions

$$J^\mu(q) = \sum_i j_i^\mu + \sum_{i < j} j_{ij}^\mu + \dots$$


The diagram shows two Feynman diagrams representing one and two-body contributions to the current operator. The first diagram shows a wavy line (representing a photon) interacting with a single nucleon (N) line. The second diagram shows a wavy line interacting with a two-body vertex (represented by a blue oval) between two nucleon (N) lines.

- ❖ Chiral Effective Field Theory Electroweak many-body currents
- ❖ “Phenomenological” Electroweak many-body currents

# Elementary Input: Form Factors



Different parametrization of the axial form factor:

Dipole: 
$$F_A(Q^2) = \frac{g_A}{(1 + Q^2/M_A^2)^2},$$

- Alternative derivation based on **z-expansion** – model independent parametrization

$$F_A(q^2) = \sum_{k=0}^{k_{\max}} a_k z(q^2)^k,$$

↑ ←  
 free parameters      known functions

Bhattacharya, Hill, and Paz PRD 84 (2011) 073006

A.S.Meyer et al, Phys.Rev.D 93 (2016) 11, 113015

D2 Meyer et al: fits to neutrino-deuteron scattering data

LQCD result: general agreement between the different calculations

LQCD results are 2-3 $\sigma$  larger than D2 Meyer ones for  $Q^2 > 0.3 \text{ GeV}^2$



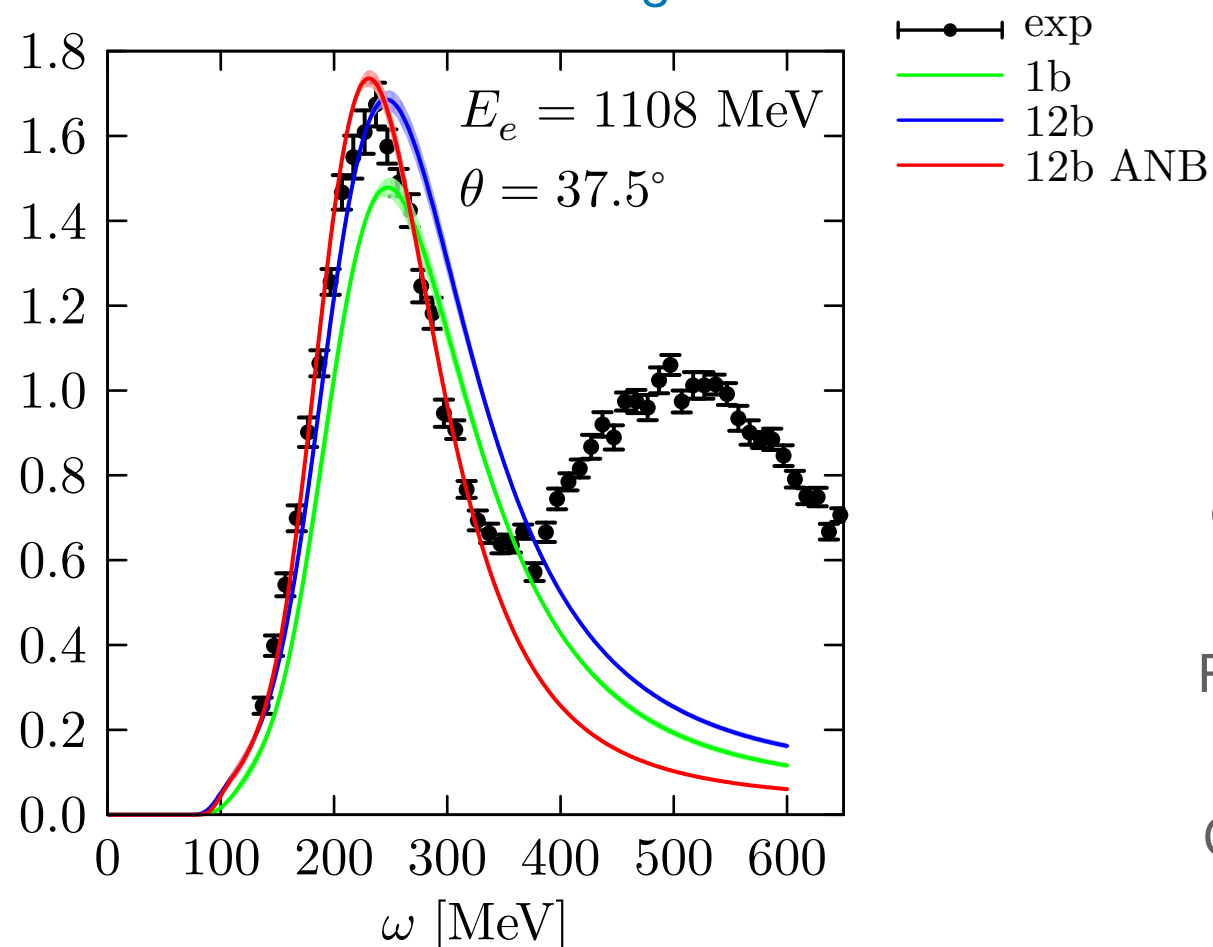
# Many-Body method: GFMC

QMC techniques projects out the exact lowest-energy state:  $e^{-(H-E_0)\tau} |\Psi_T\rangle \rightarrow |\Psi_0\rangle$

This approach accounts for all the possible interactions and correlations effects between nucleons in both the initial and final nucleus.

Computationally very expensive, scales exponentially with the number of particles, limited to  $^{12}\text{C}$ .

—electron- $^4\text{He}$  scattering



[A. Lovato et al, PRL117 \(2016\), 082501](#)

[A. Lovato et al, PRC97 \(2018\), 022502](#)

**Inclusive** results which are **virtually exact** in the QE

Different Hamiltonians can be used in the time-evolution operator

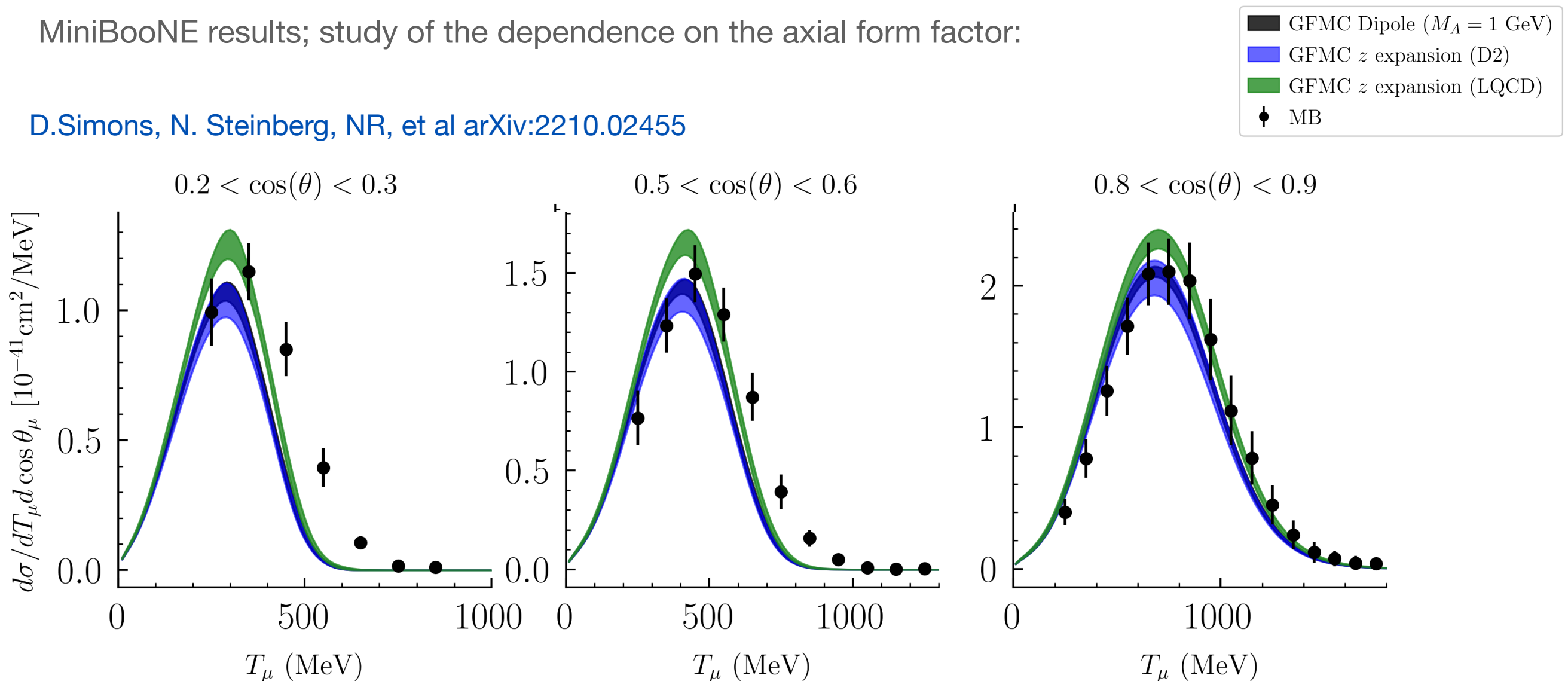
Relies on non-relativistic treatment of the kinematics

Can not handle explicit pion degrees of freedom

# Study of model dependence in neutrino predictions

MiniBooNE results; study of the dependence on the axial form factor:

D.Simons, N. Steinberg, NR, et al arXiv:2210.02455



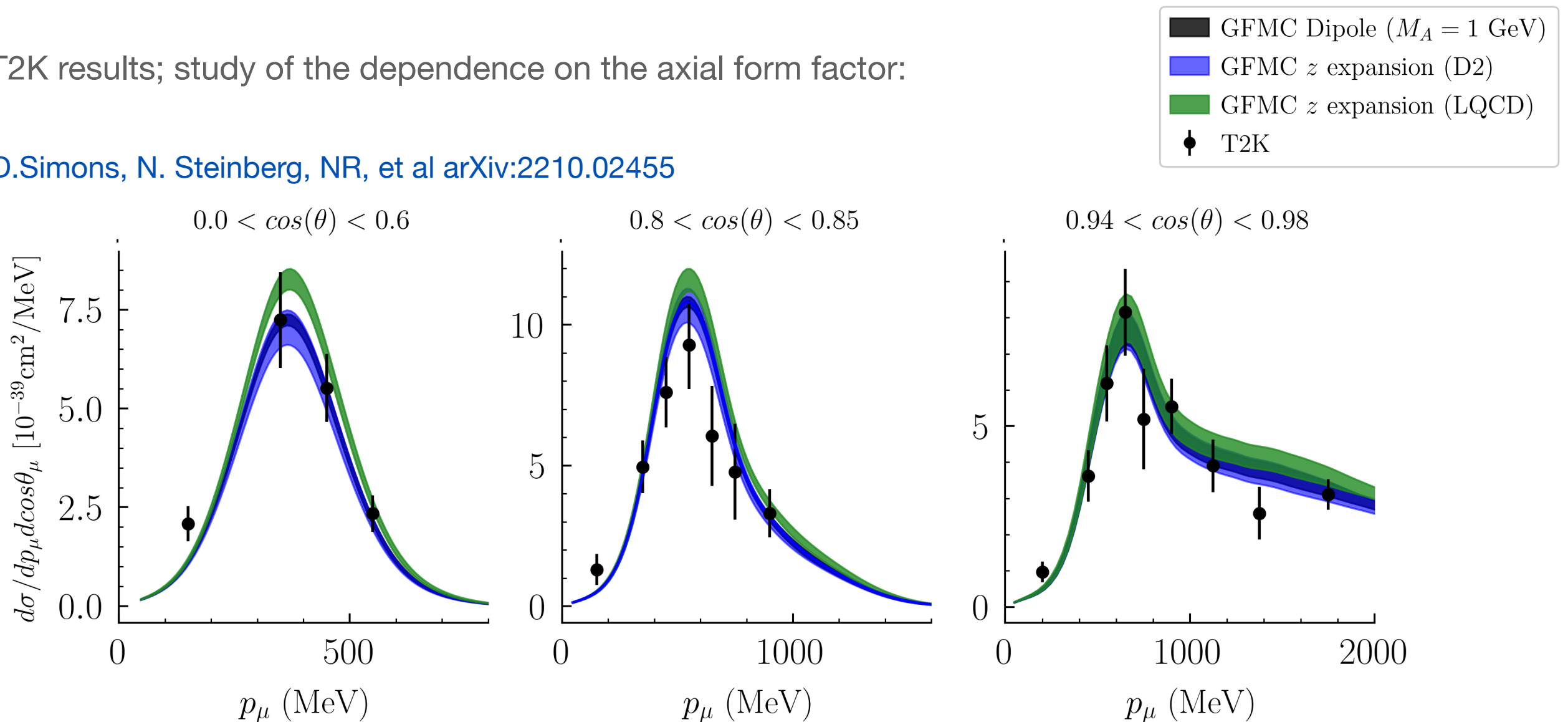
D.Simons, N. Steinberg et al, 2210.02455

MiniBooNE	$0.2 < \cos \theta_\mu < 0.3$	$0.5 < \cos \theta_\mu < 0.6$	$0.8 < \cos \theta_\mu < 0.9$
GFMC Difference in $d\sigma_{\text{peak}}$ (%)	18.6	17.1	12.2

# Study of model dependence in neutrino predictions

T2K results; study of the dependence on the axial form factor:

D.Simons, N. Steinberg, NR, et al arXiv:2210.02455



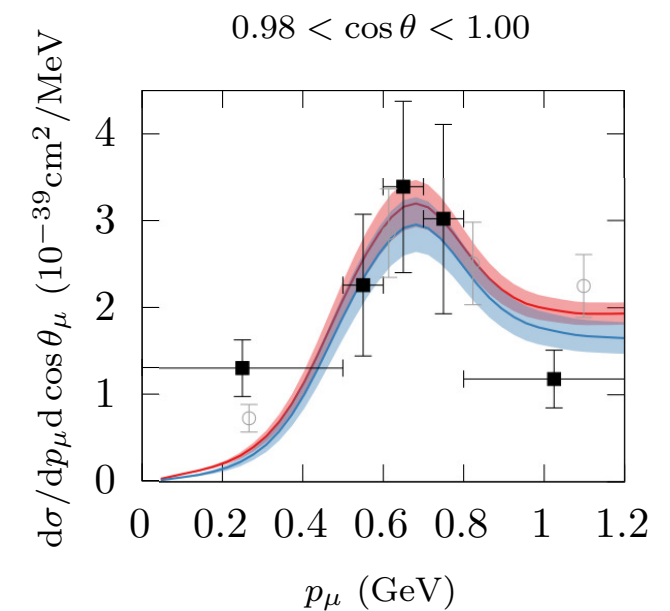
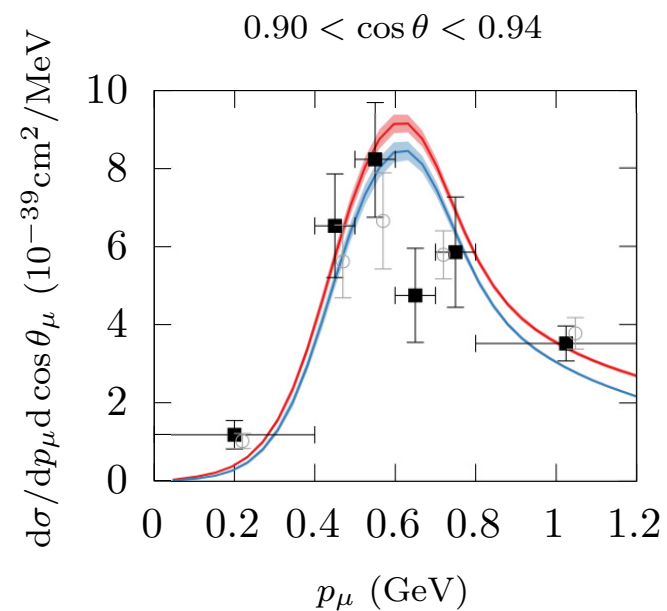
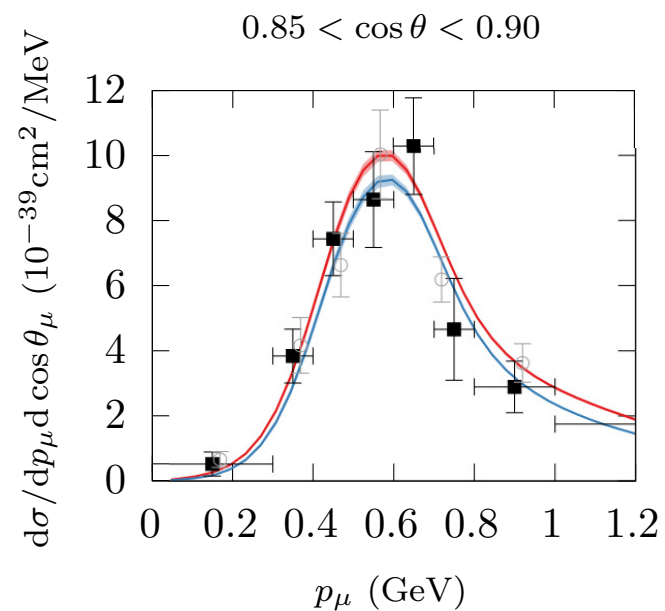
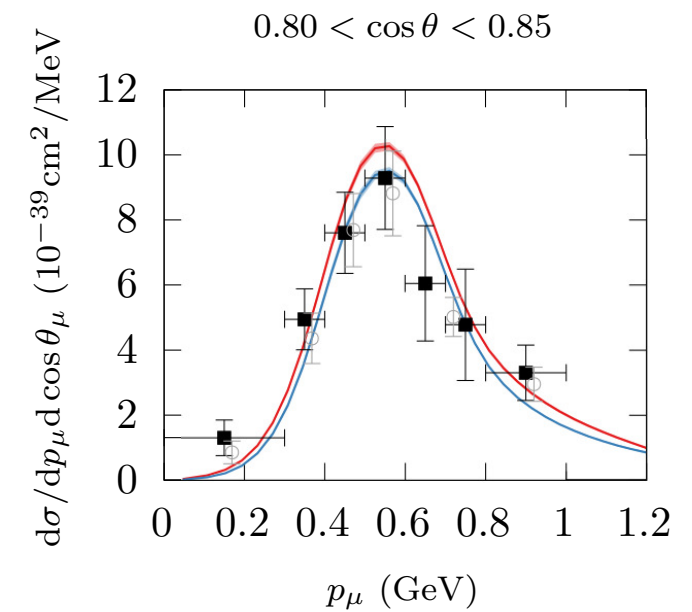
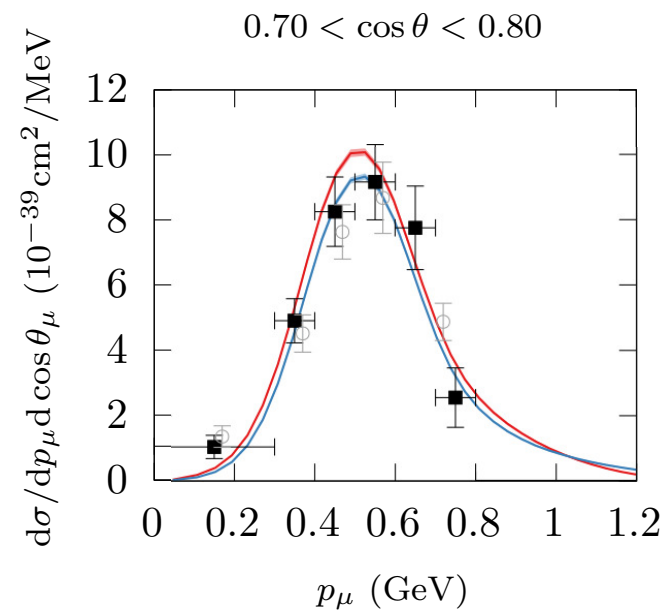
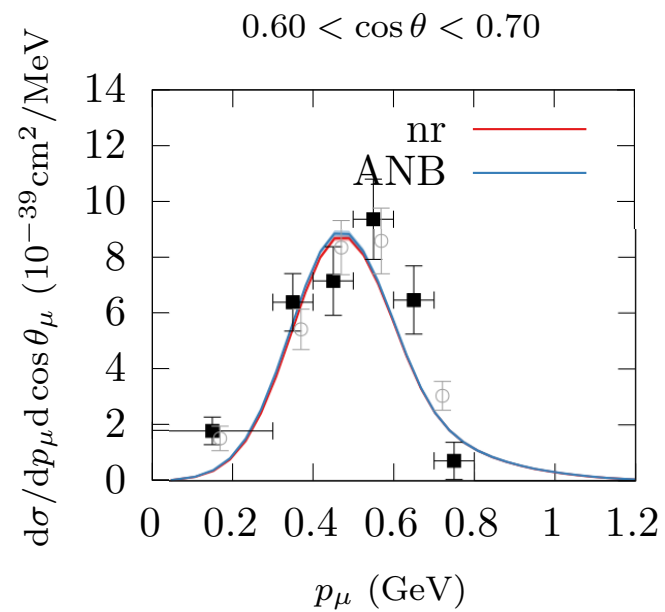
D.Simons, N. Steinberg et al, 2210.02455

T2K	$0.0 < \cos \theta_\mu < 0.6$	$0.80 < \cos \theta_\mu < 0.85$	$0.94 < \cos \theta_\mu < 0.98$
GFMC difference in $d\sigma_{\text{peak}}$ (%)	15.8	8.0	4.6

# Cross sections: Green's Function Monte Carlo

T2K results including relativistic corrections

A.Nikolakopoulos, A.Lovato, NR, arXiv:2304.11772

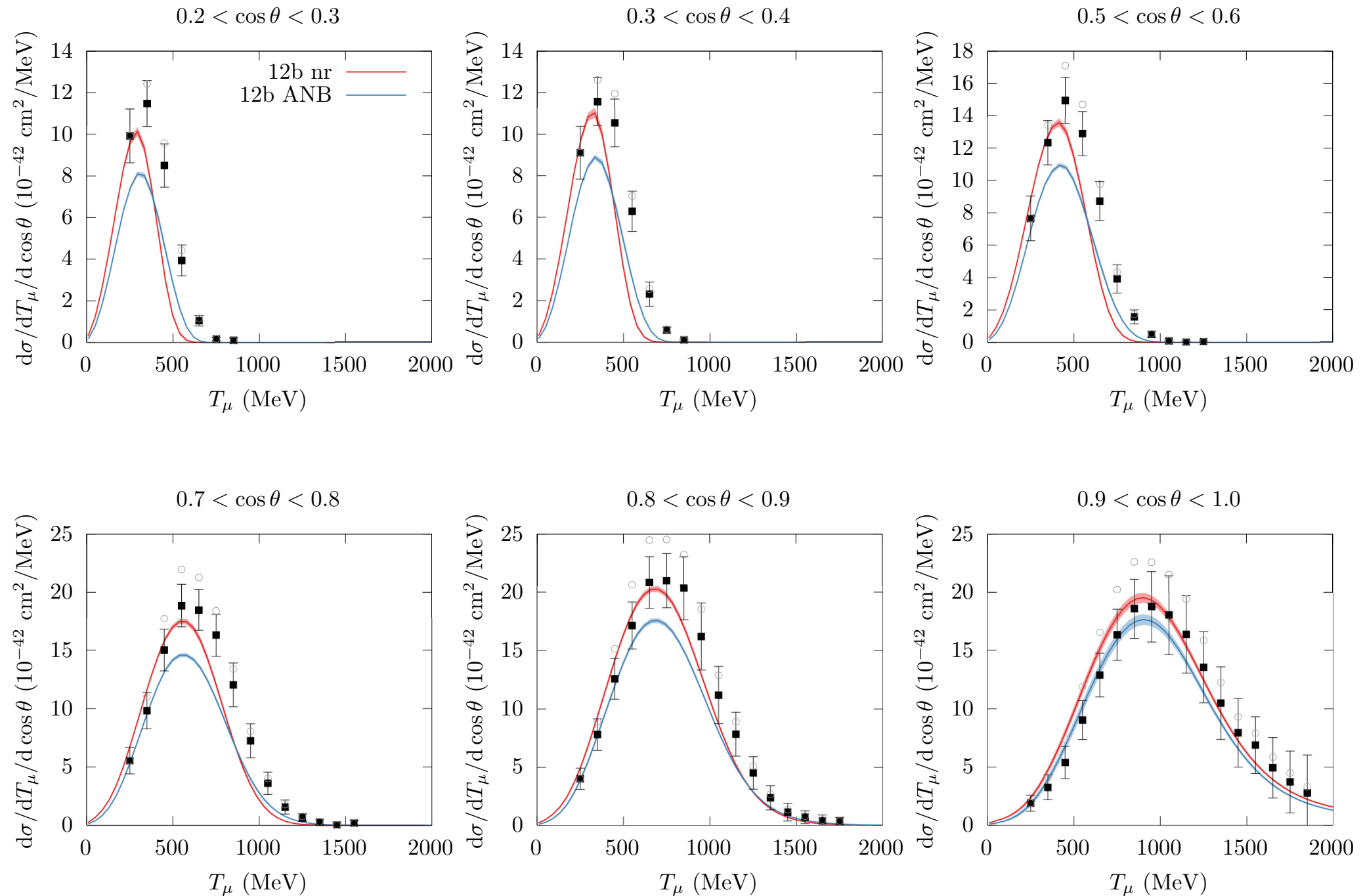




# Cross sections: Green's Function Monte Carlo

MiniBooNE results including relativistic corrections

A.Nikolakopoulos, A.Lovato, NR, arXiv:2304.11772



# Coupled Cluster Method

Reference state Hartree Fock:  $|\Psi\rangle$

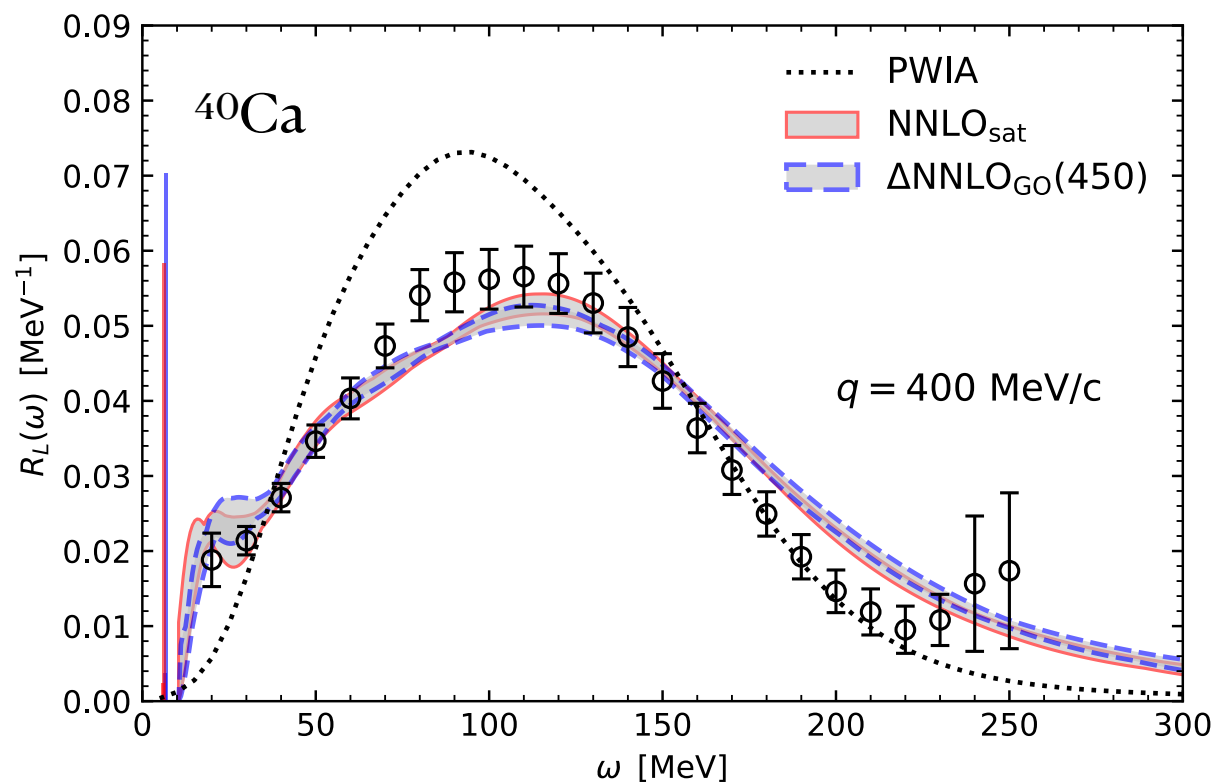
Include correlations through  $e^T$  operator

Similarity transformed Hamiltonian  $e^{-T} H e^T |\Psi\rangle = \bar{H} |\Psi\rangle = E |\Psi\rangle$

Expansion in second quantization single + doubles:

$$T = \sum t_a^i a_a^\dagger a_i + \sum t_{ab}^{ij} a_a^\dagger a_b^\dagger a_i a_j + \dots$$

Coefficients are obtained using coupled cluster equations



Polynomial scaling with the number of nucleons (predictions for  $^{132}\text{Sn}$  and  $^{208}\text{Pb}$ )

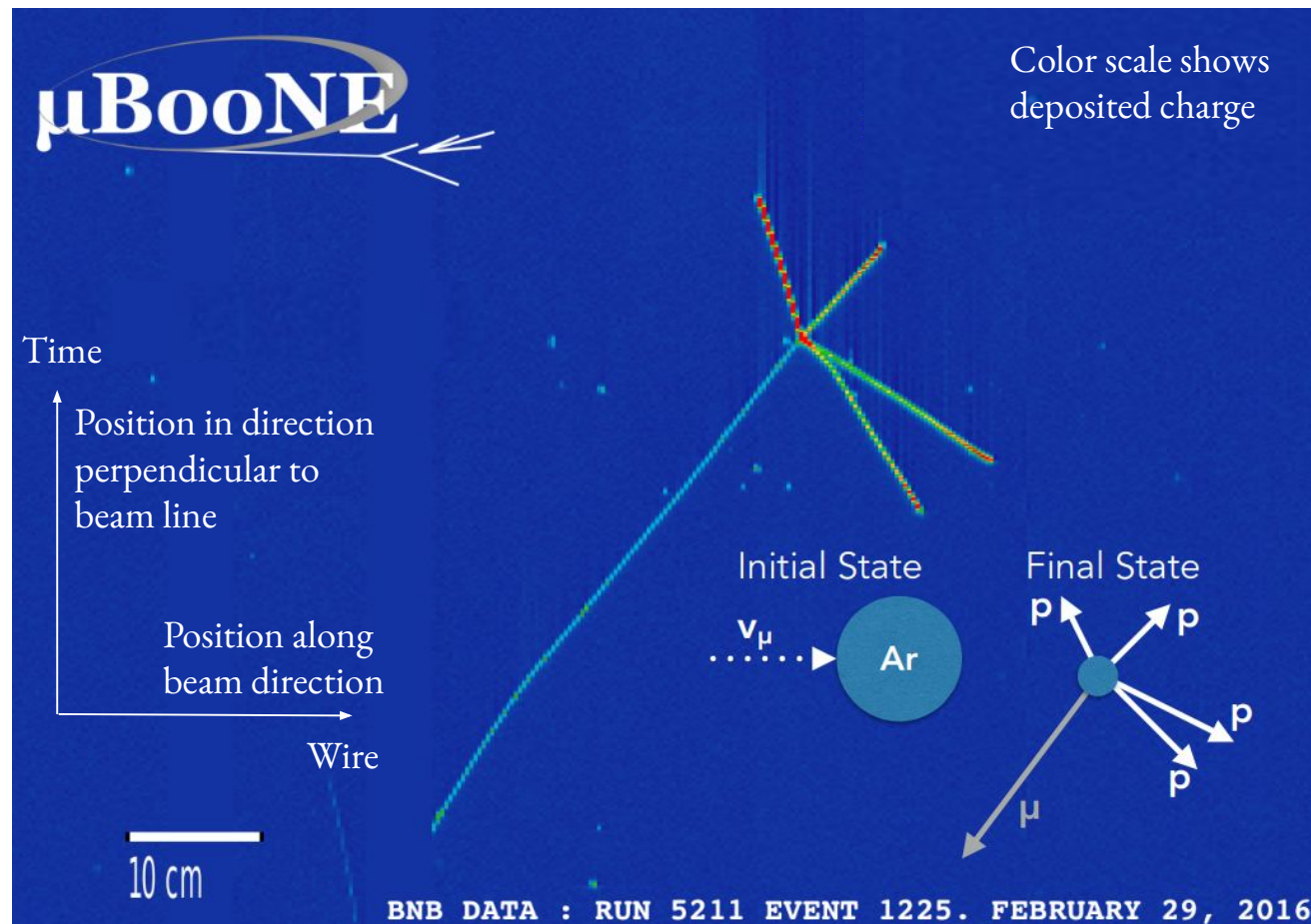
Limited to the low energy region - requires inversion procedure

- Extension of this approach to higher energies: use CC to derive nuclear spectral functions

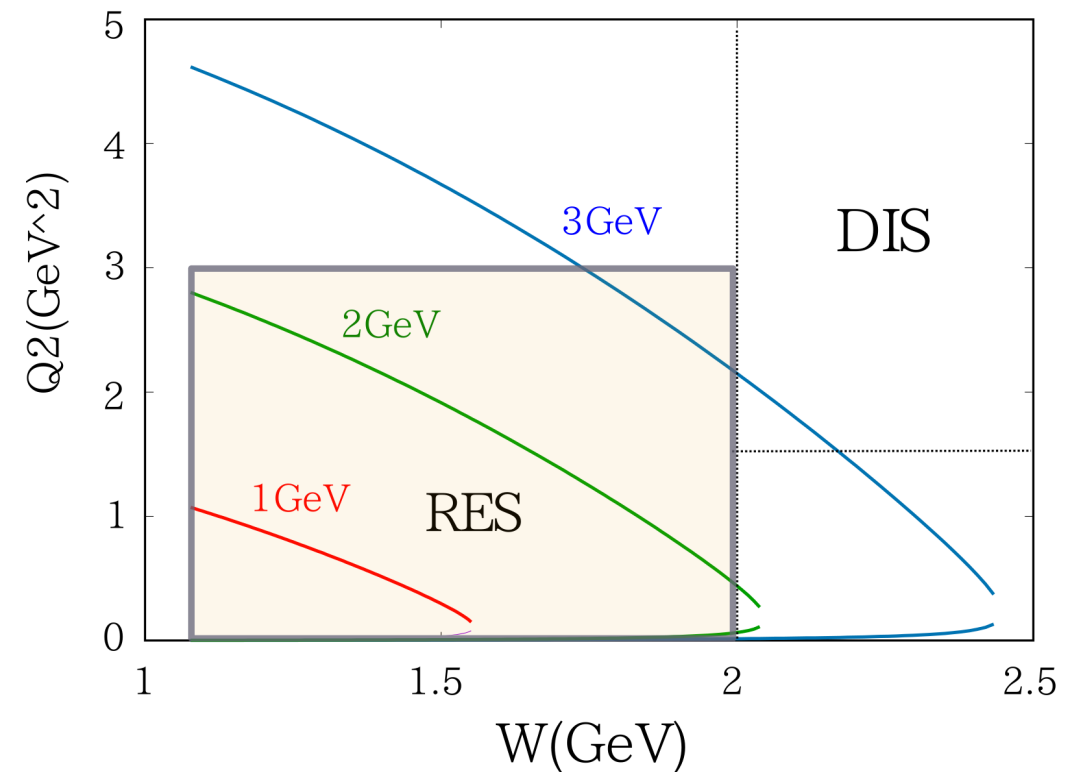
J. E. Sobczyk, B. Acharya, et al ; PRL 127 (2021) 7, 072501

J. E. Sobczyk, S Bacca arXiv:2309.00355

# Address new experimental capabilities



T.Sato talks @ NuSTEC Workshop on Neutrino-Nucleus Pion Production in the Resonance Region

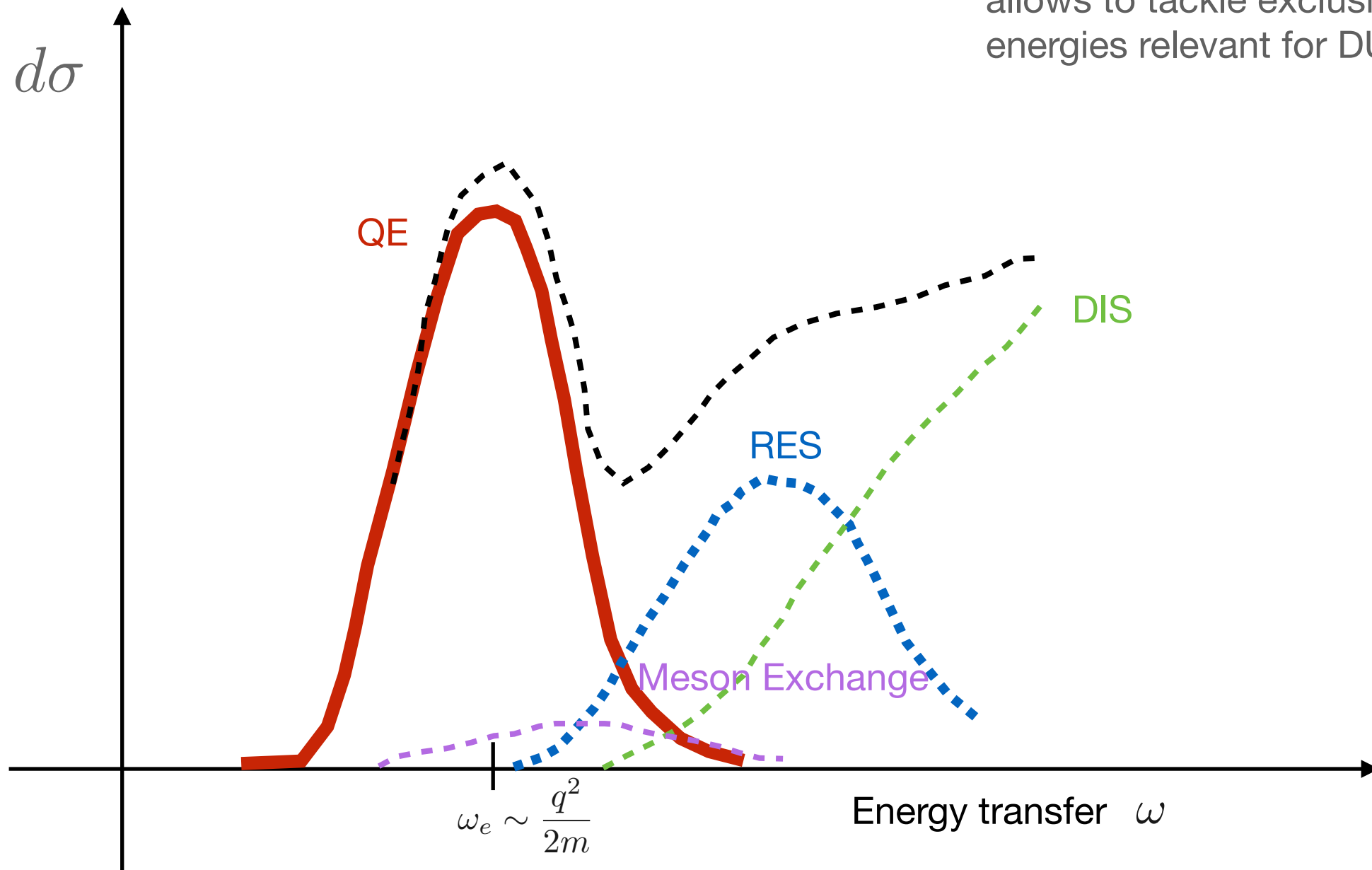


- Excellent spatial resolution
- Precise calorimetric information
- Powerful particle identification

$$W = \sqrt{(p + q)^2}, Q^2 = -q^2 = -(p_\nu - p_l)^2$$

# Factorization Based Approaches

Factorization of the hadronic final states:  
allows to tackle exclusive channels + higher  
energies relevant for DUNE

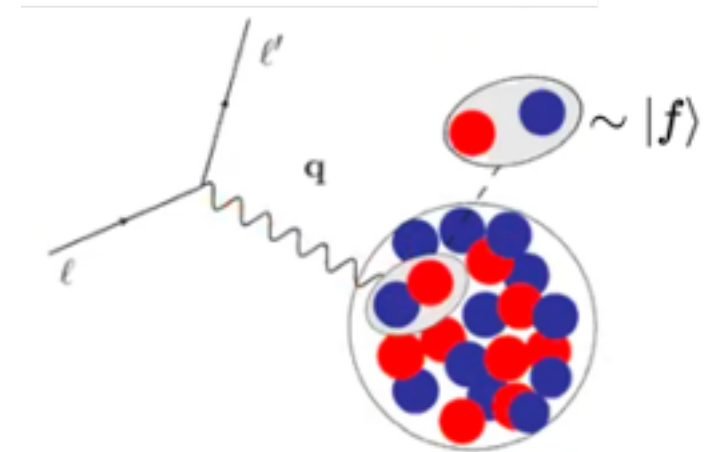




# Short-Time Approximation

S. Pastore et al ; PRC1 01(2020)044612

- ❖ Based on factorization retains two-body physics
- ❖ Response functions are given by the scattering from pairs of fully interacting nucleons that propagate into a correlated pair of nucleons
- ❖ Allows to retain both two-body correlations and currents at the vertex
- ❖ Provides “more” exclusive information in terms of nucleon-pair kinematics via the Response Densities



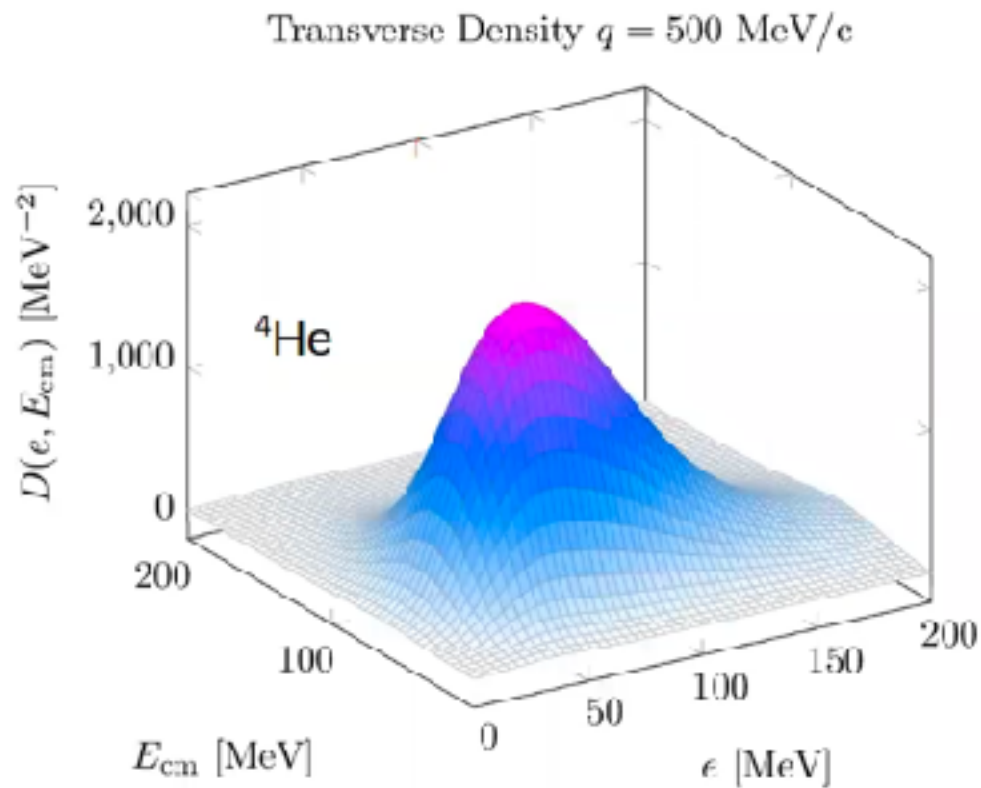
The sum over all final states is replaced by a two nucleon propagator

$$R_{\alpha}(q, \omega) = \int_{-\infty}^{\infty} \frac{dt}{2\pi} e^{i(\omega + E_i)t} \langle \Psi_i | O_{\alpha}^{\dagger}(\mathbf{q}) e^{-iHt} O_{\alpha}(\mathbf{q}) | \Psi_i \rangle$$

The STA restricts the propagation to two active nucleons and allows to compute density functions of the CoM and relative momentum of the pair

$$R^{\text{STA}}(q, \omega) \sim \int \delta(\omega + E_0 - E_f) de dE_{cm} \mathcal{D}(e, E_{cm}; q)$$

# Short-Time Approximation



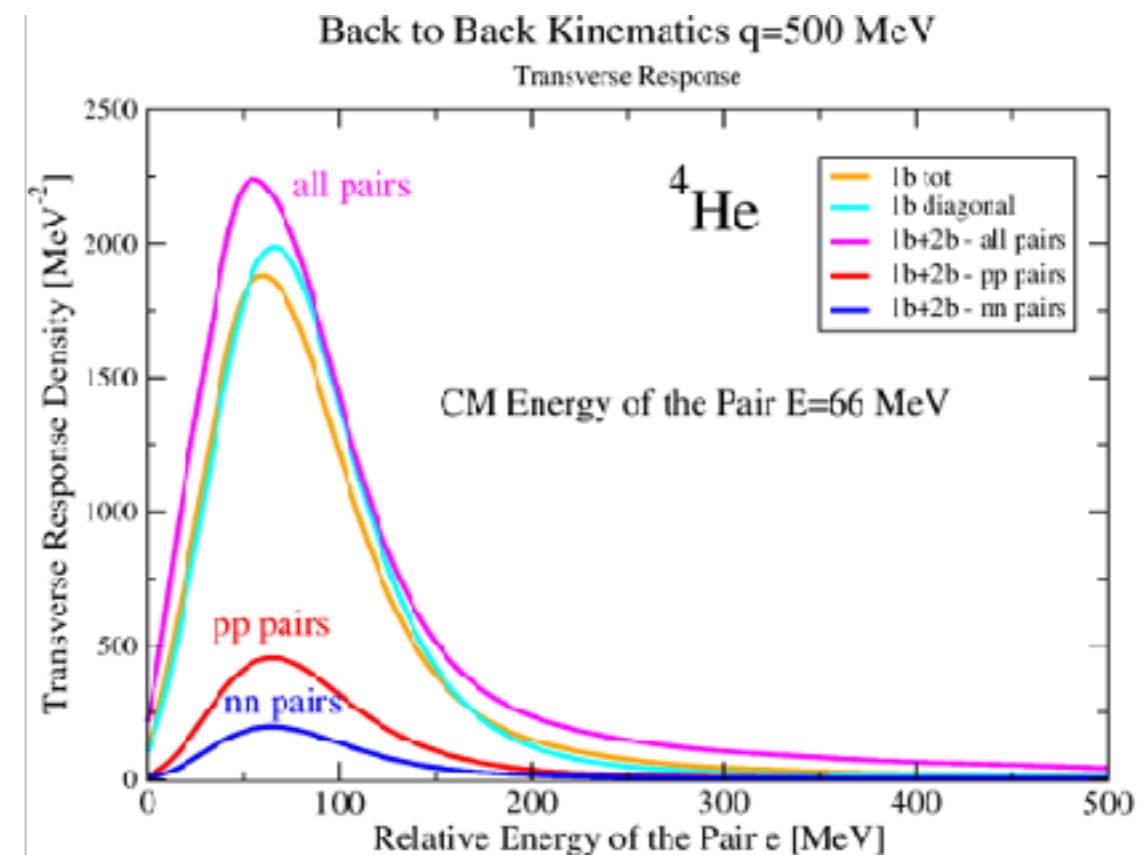
S. Pastore et al ; PRC1 01(2020)044612

- **pp pairs**
- **nn pairs**
- **1 body tot**
- **all pairs tot**

$$R^{\text{STA}}(q, \omega) \sim \int \delta(\omega + E_0 - E_f) de dE_{cm} \mathcal{D}(e, E_{cm}; q)$$

Electron scattering from  $^4\text{He}$ :

- ❖ Response density as a function of  $(E, e)$
- ❖ Give access to particular kinematics for the struck nucleon pair



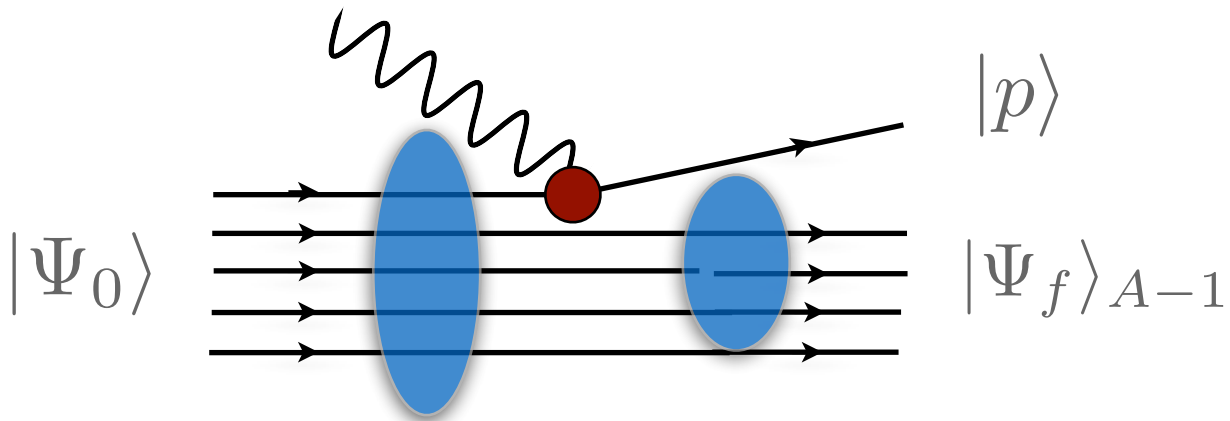
# Spectral function approach

At large momentum transfer, the scattering reduces to the sum of individual terms

$$J_\alpha = \sum_i j_\alpha^i \quad |\Psi_f\rangle \rightarrow |p\rangle \otimes |\Psi_f\rangle_{A-1}$$

The incoherent contribution of the one-body response reads

$$R_{\alpha\beta} \simeq \int \frac{d^3k}{(2\pi)^3} dE P_h(\mathbf{k}, E) \sum_i \langle k | j_\alpha^{i\dagger} | k + q \rangle \langle k + q | j_\beta^i | k \rangle \delta(\omega + E - e(\mathbf{k} + \mathbf{q}))$$



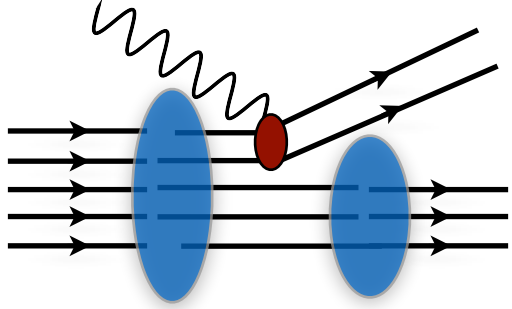
The Spectral Function is the imaginary part of the two point Green's Function

Different many-body methods can be adopted to determine it

I. Korover, et al Phys.Rev.C 107 (2023) 6, L061301  
 O. Benhar et al, Rev.Mod.Phys. 80 (2008)  
 NR, Frontiers in Phys. 8 (2020) 116

# Spectral function approach

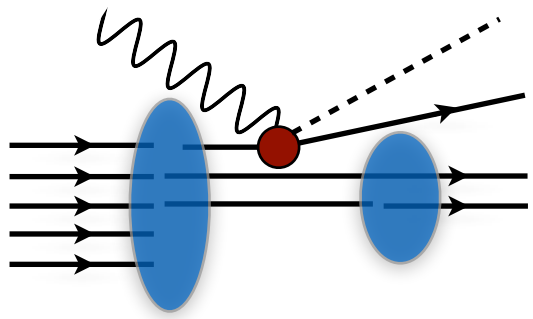
$$|f\rangle \rightarrow |pp'\rangle_a \otimes |f_{A-2}\rangle$$



The hadronic tensor for two-body current factorizes as

$$R_{2b}^{\mu\nu}(\mathbf{q}, \omega) \propto \int dE d^3k d^3k' P_{2b}(\mathbf{k}, \mathbf{k}', E) \times d^3p d^3p' |\langle kk' | j_{2b}^\mu | pp' \rangle|^2$$

$$|f\rangle \rightarrow |p_\pi p\rangle \otimes |f_{A-1}\rangle$$



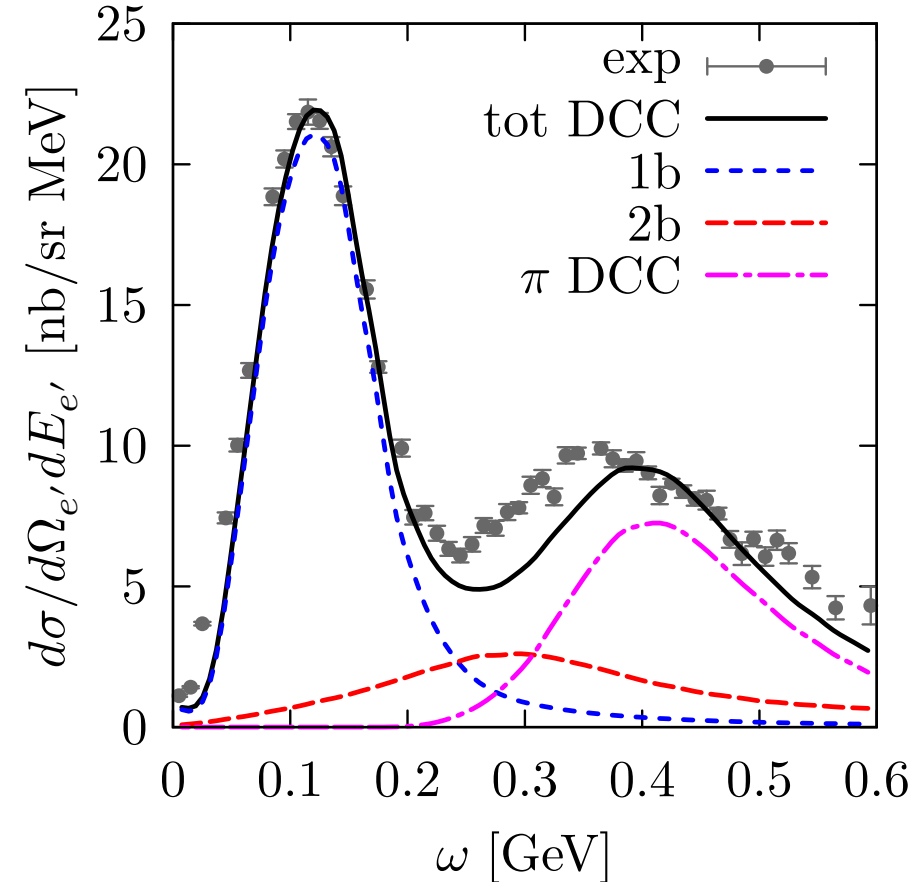
Production of real  $\pi$  in the final state

$$R_{1b\pi}^{\mu\nu}(\mathbf{q}, \omega) \propto \int dE d^3k P_{1b}(\mathbf{k}, E) \times d^3p d^3k_\pi |\langle k | j^\mu | pk_\pi \rangle|^2$$

\* Pion production elementary amplitudes currently derived within the extremely sophisticated **Dynamic Couple Chanel approach**;

S.X.Nakamura, et al PRD92(2015)  
T. Sato, et al PRC67(2003)

$E_e = 730 \text{ MeV}, \theta_e = 37.0^\circ$



NR, Frontiers in Phys. 8 (2020) 116

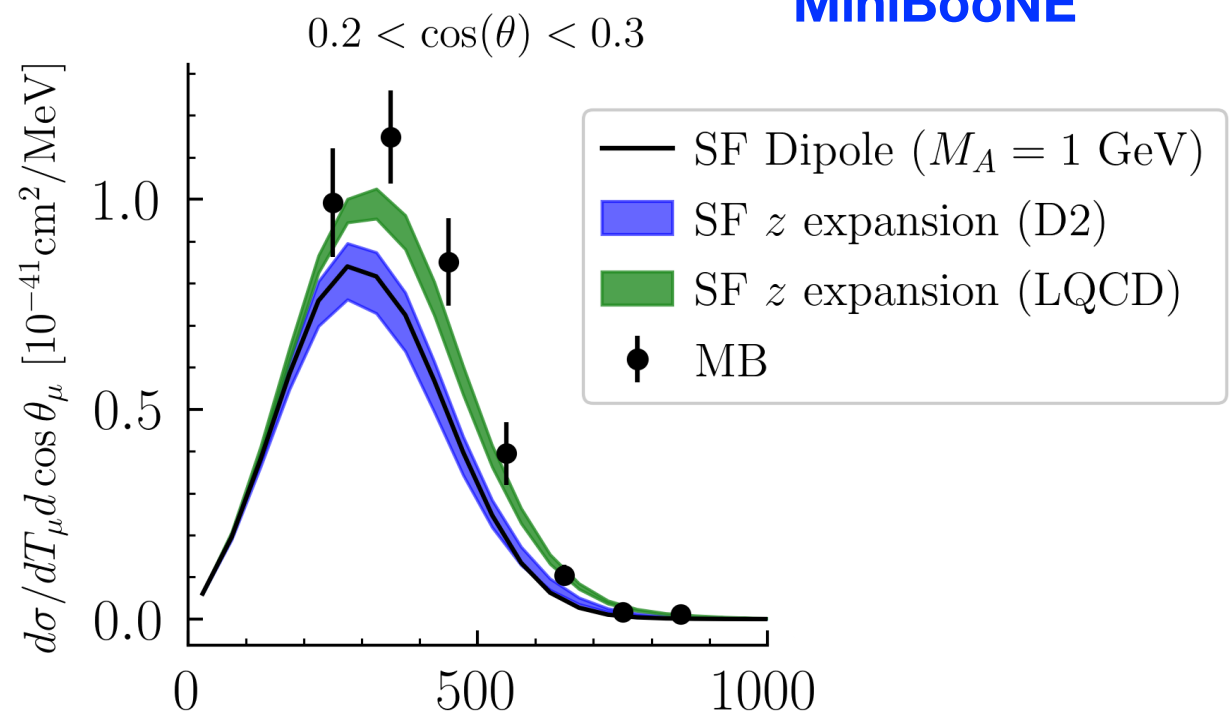




# Axial Form Factors Uncertainty needs

## MiniBooNE

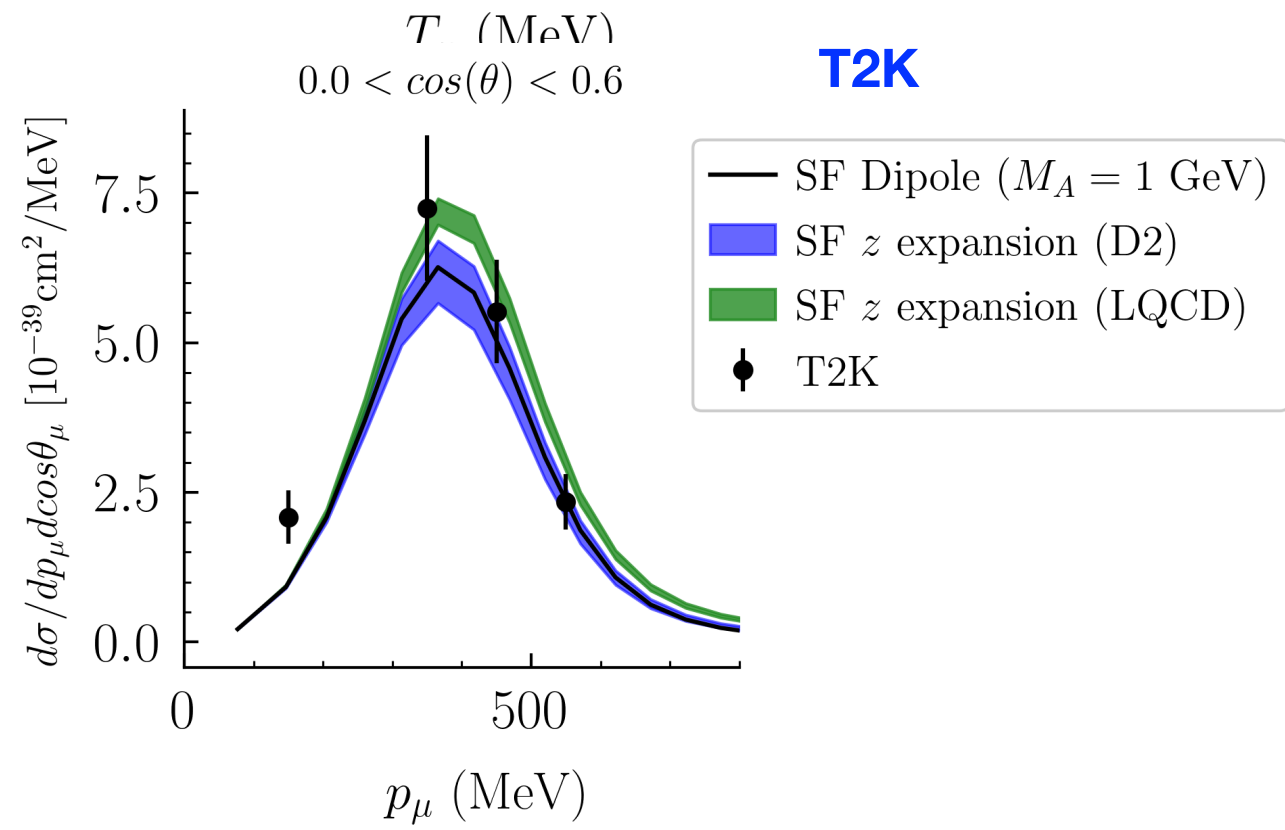
D.Simons, N. Steinberg et al, 2210.02455



\* Axial form factor dependence:

MiniBooNE	0.2 < $\cos\theta_\mu$ < 0.3
SF Difference in $d\sigma_{\text{peak}}$ (%)	16.3

## T2K



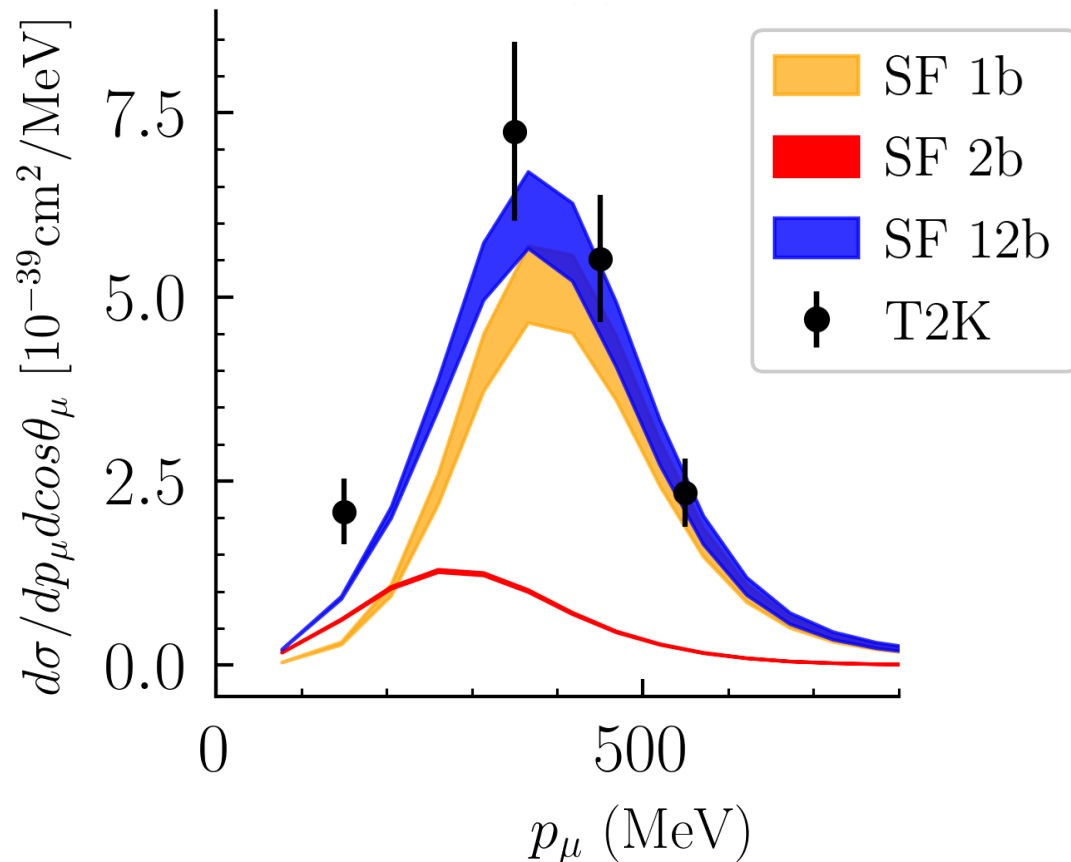
\* Axial form factor dependence:

T2K	0.0 < $\cos\theta_\mu$ < 0.6
SF difference in $d\sigma_{\text{peak}}$ (%)	15.3

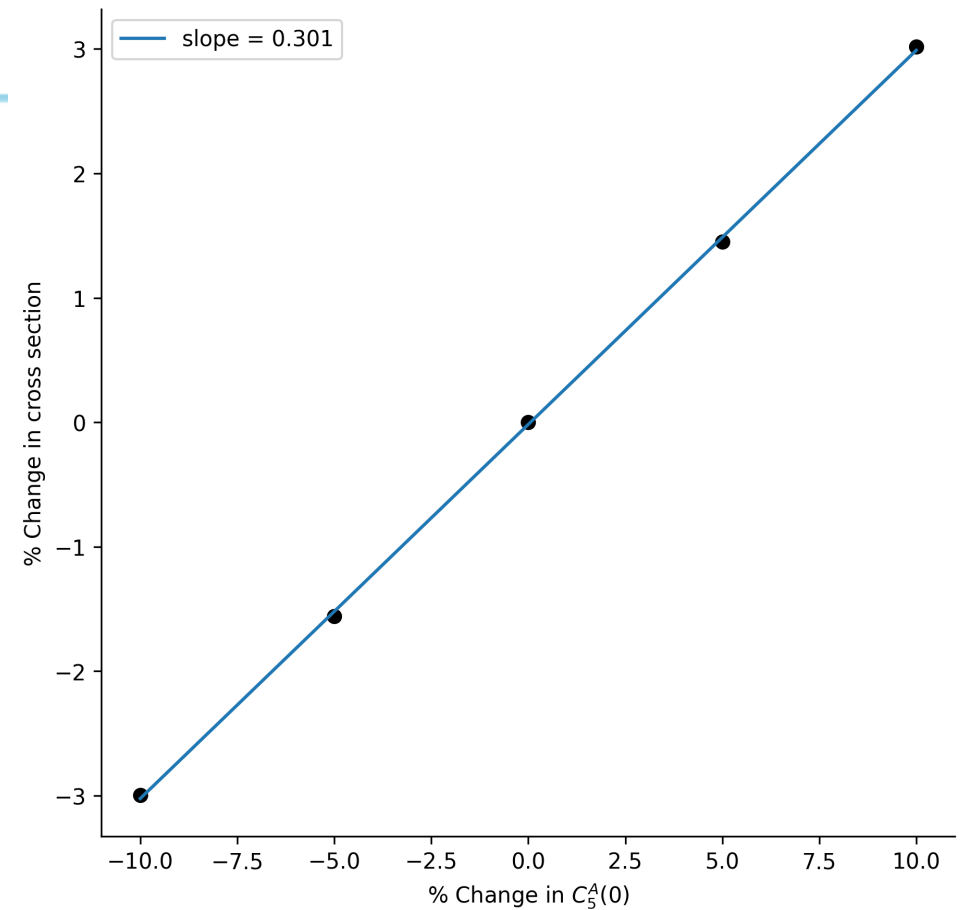


# Resonance Uncertainty needs

The largest contributions to two-body currents arise from resonant  $N \rightarrow \Delta$  transitions yielding pion production



D.Simons, N. Steinberg et al, 2210.02455



The normalization of the dominant  $N \rightarrow \Delta$  transition form factor needs to be known to 3% precision to achieve 1% cross-section precision for MiniBooNE kinematics

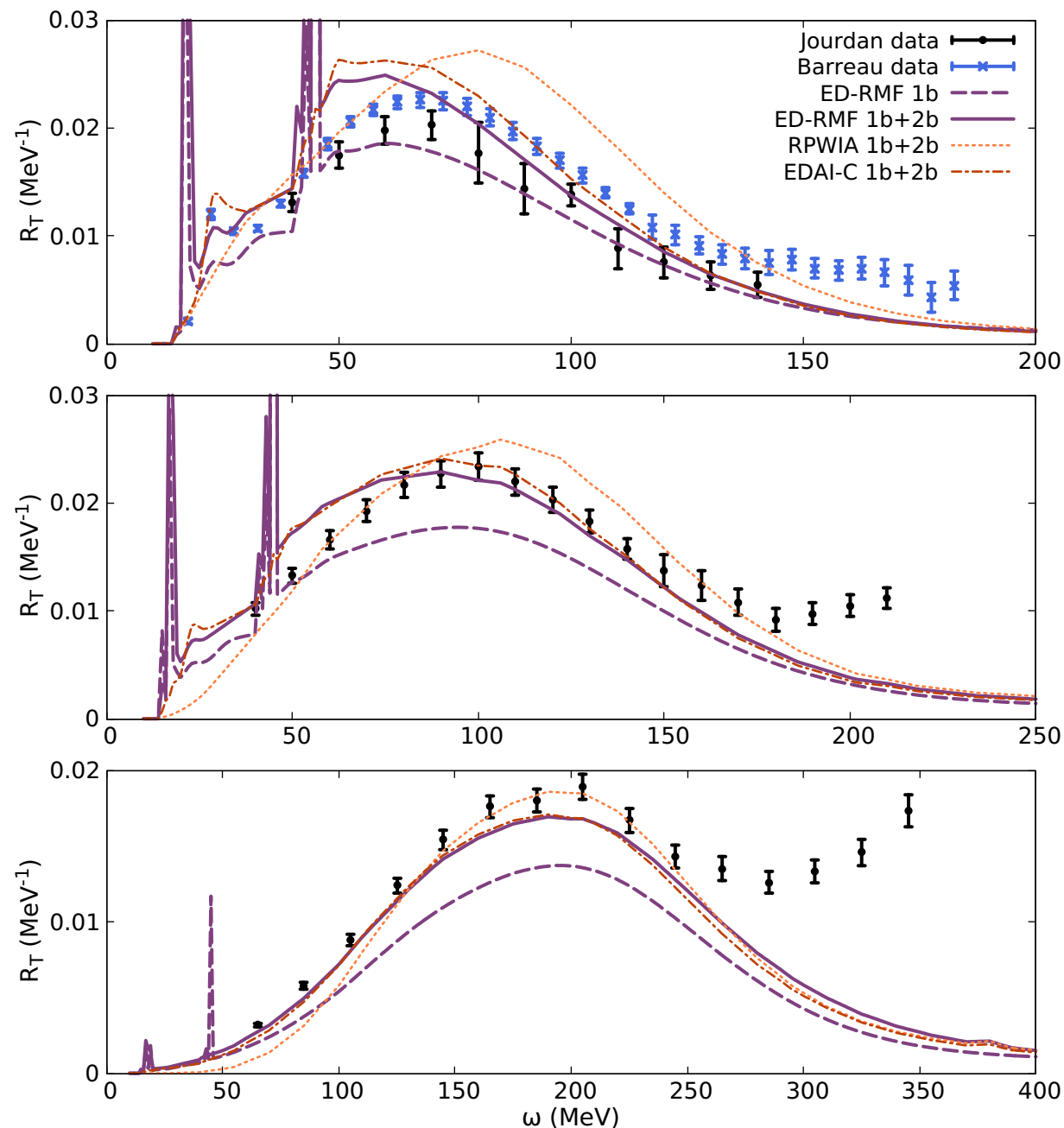
State-of-the-art determinations of this form factor from experimental data on pion electroproduction achieve **10-15% precision** (under some assumptions)

[Hernandez et al, PRD 81 \(2010\)](#)

Further constraints on  $N \rightarrow \Delta$  transition relevant for two-body currents and  $\pi$  production will be necessary to achieve few-percent cross-section precision

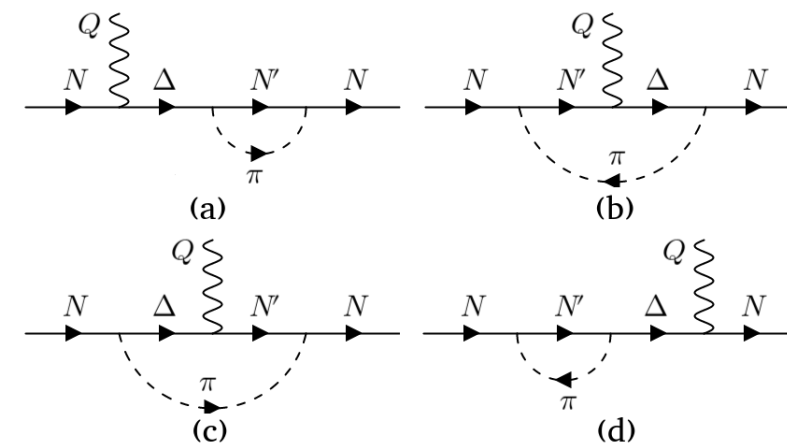
# Effects of two-body currents within a RMF approach

T. Franco-Munoz, R. Gonzalez-Jimenez, and J.M. Udias, arXiv: 2203.09996



Hadronic current, with bound wave function obtained within a RMF approach

$$J_{\kappa, m_j, s}^{\mu} \propto \int d\mathbf{p} \bar{\Psi}^s(\mathbf{p} + \mathbf{q}, \mathbf{p}_N) \mathcal{O}^{\mu} \Psi_{\kappa}^{m_j}(\mathbf{p}).$$



**Significant enhancement** coming from **interference** between one- and two-body currents contributing in the quasielastic region

# One- and two-body current interference

Interference effects between **one-** and **two-body currents** yielding **single nucleon knock-out**

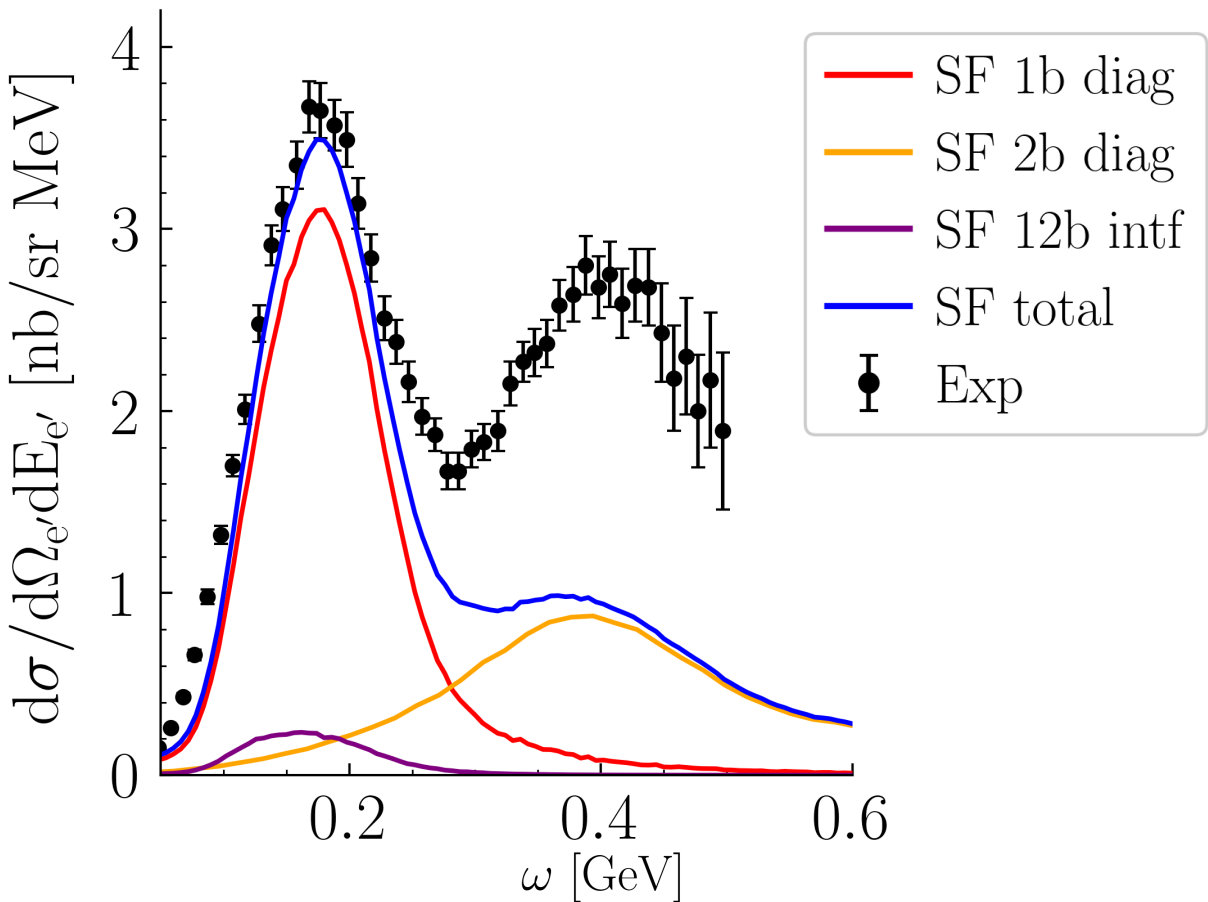
This contribution has been recently included in the spectral function formalism

Observe an enhancement in the quasi elastic region in electron and neutrino scattering

N. Steinberg, NR, A. Lovato, in preparation

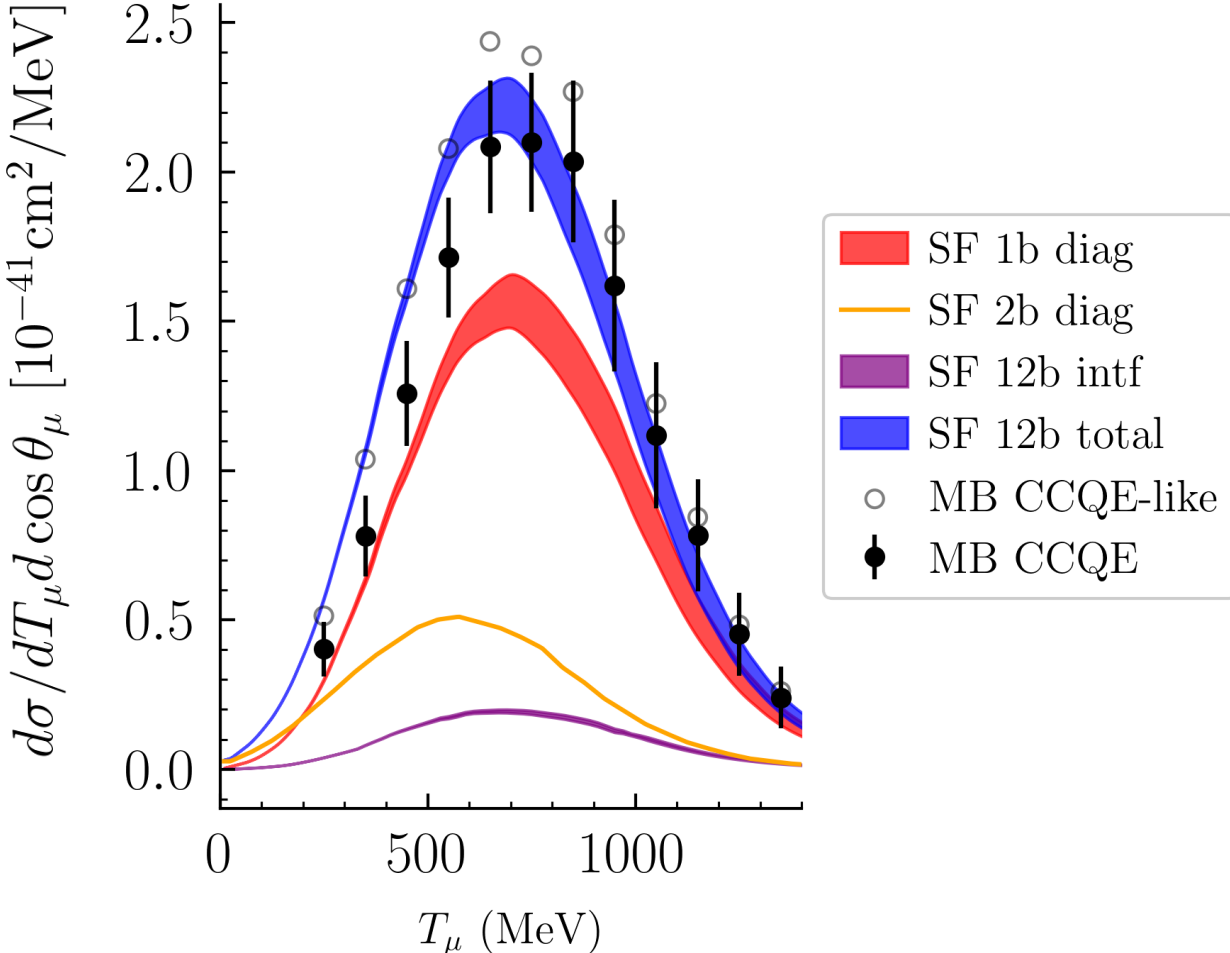
- electron-12C

$E_e = 620 \text{ MeV}, \theta_{e'} = 60.0^\circ$



$-\nu_\mu -^{12}\text{C}$  flux folded

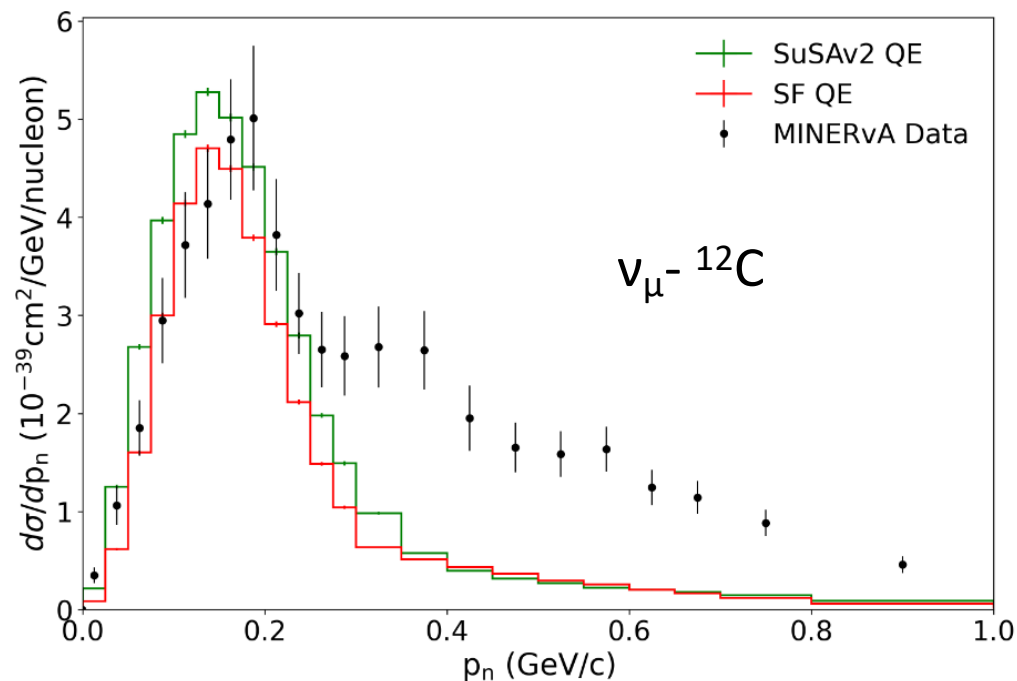
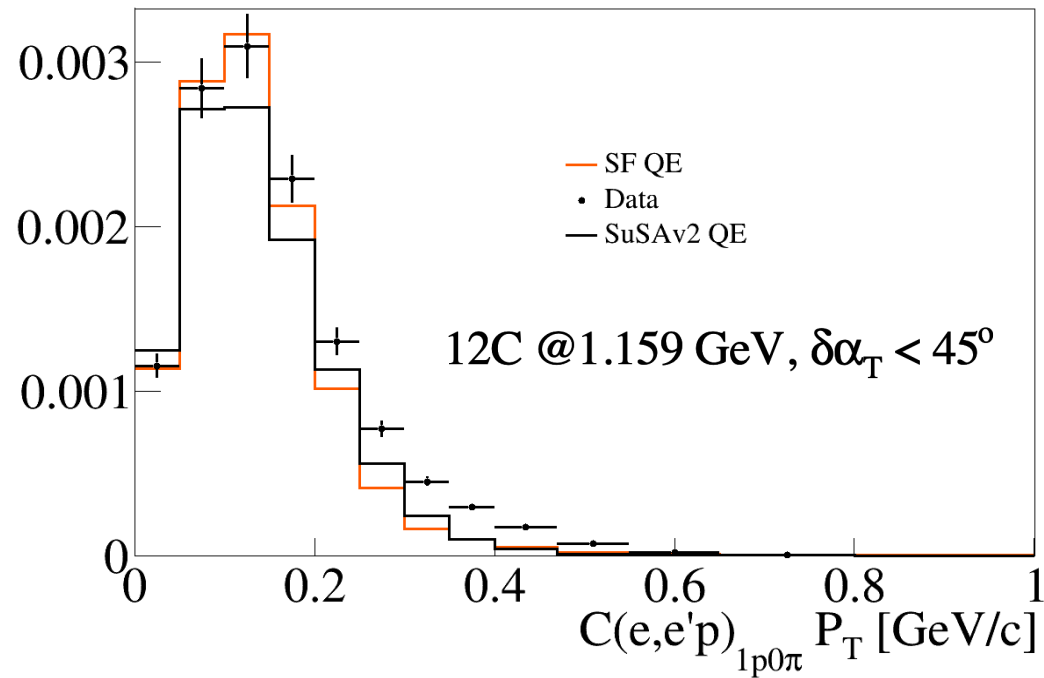
$0.8 < \cos(\theta) < 0.9$



# Implementation in event generators

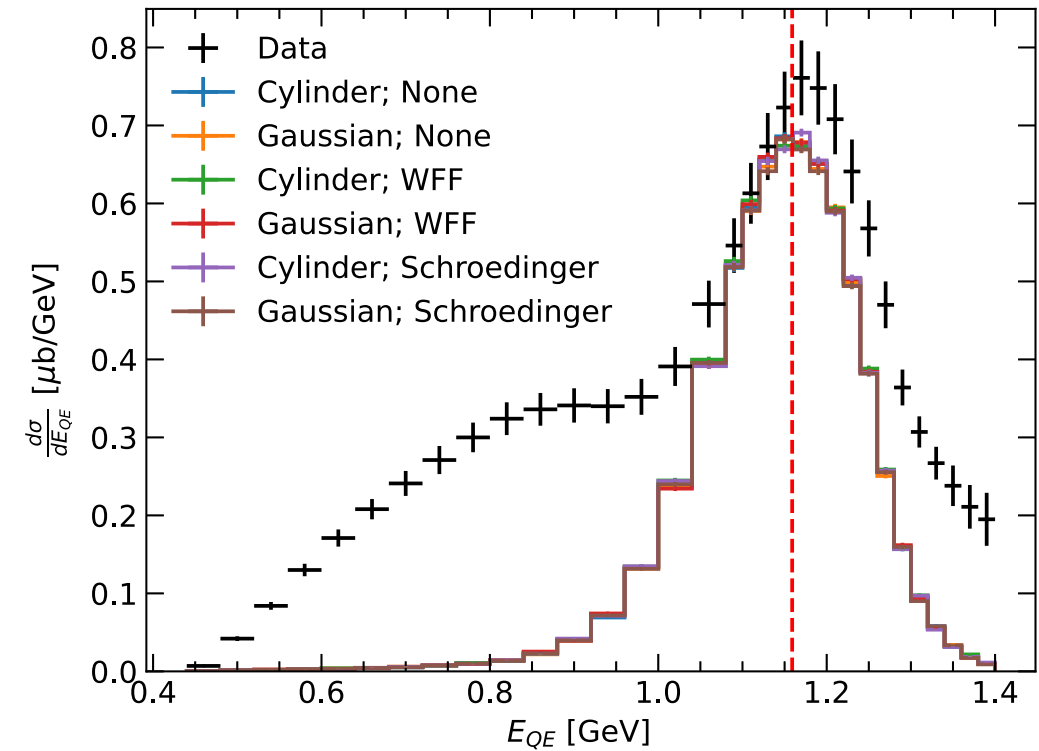
## Implementation into GENIE event generator

N. Steinberg, NR, et al, arXiv 2308.15524

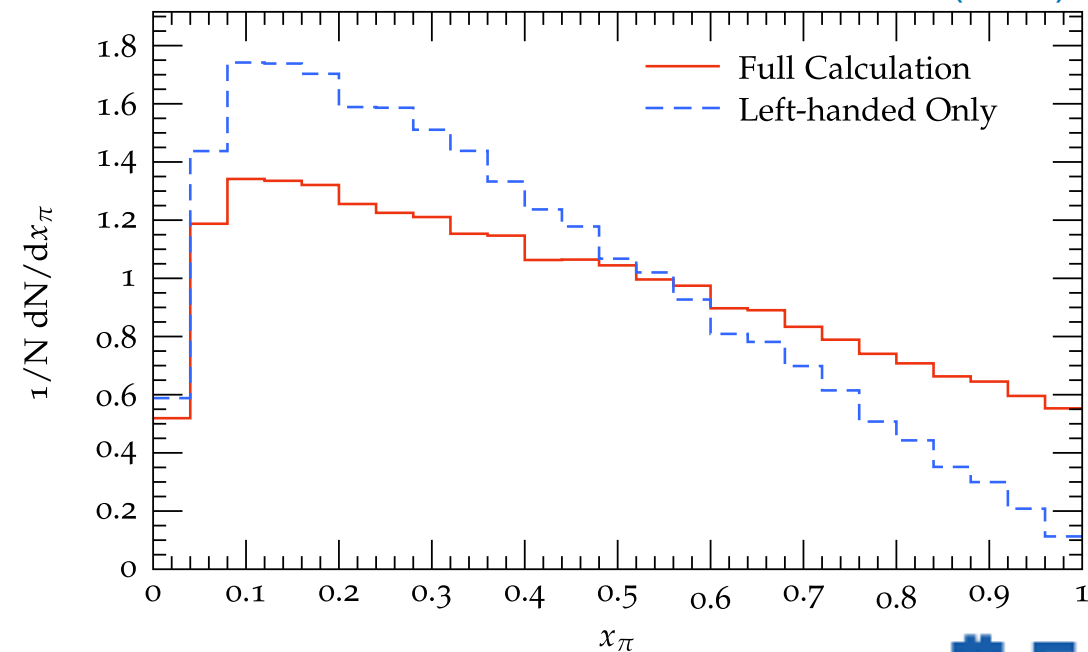


## Implementation into Achilles event generator

J. Isaacson, NR, et al, PRD 107 (2023) 3, 033007

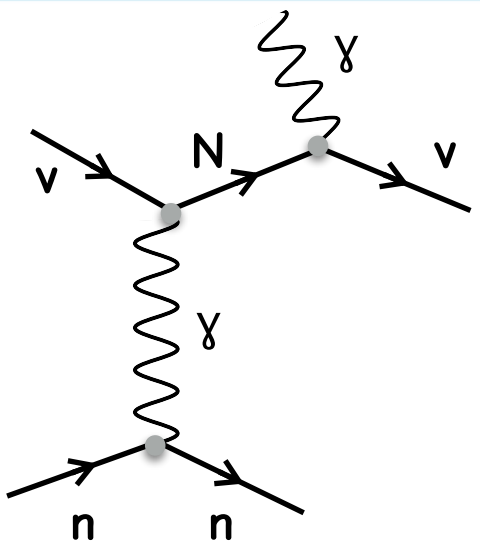
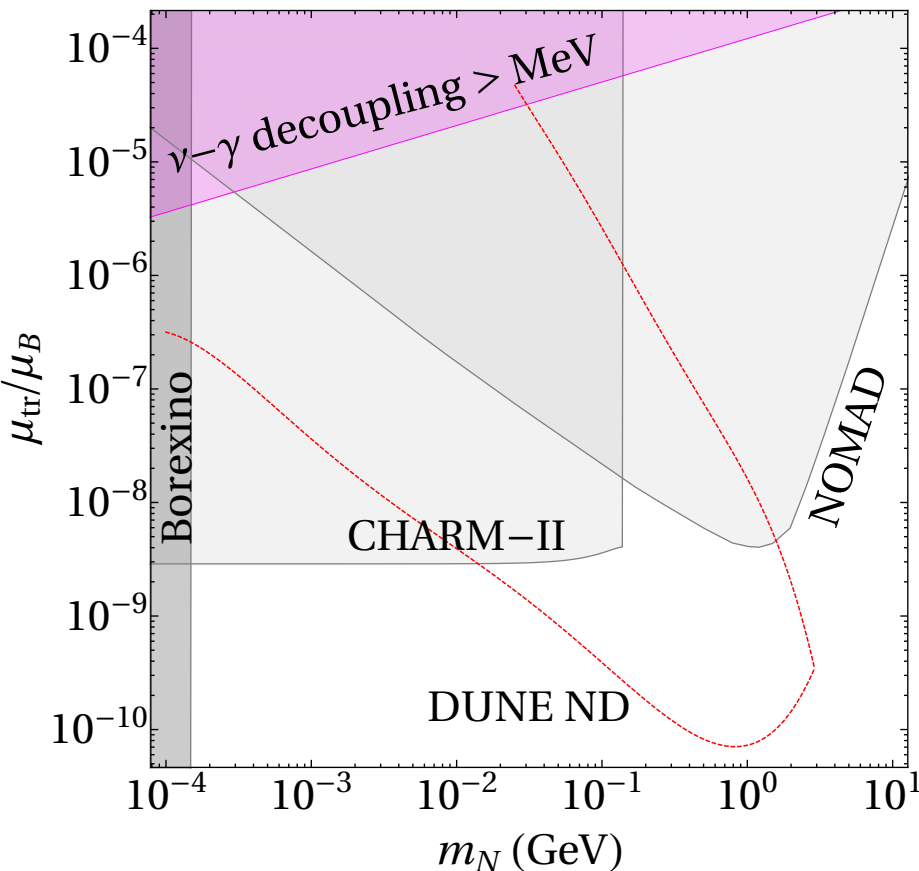


J. Isaacson, et al, PRD 108 (2023) 9, 093004





# Interplay with BSM scenarios

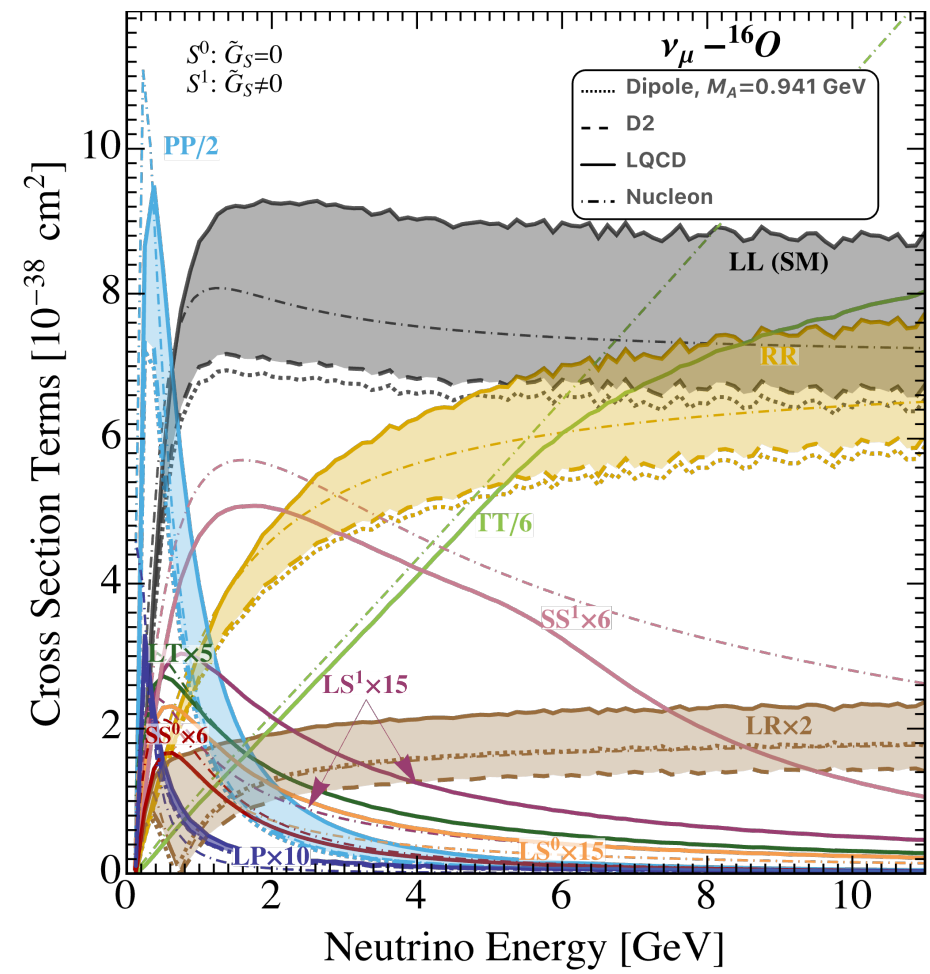


- Production via magnetic moment; nuclear target described within the spectral function
- Expected sensitivity to the **transition magnetic moment  $\nu_\mu - N$**  from **DBs** signals in the DUNE LAr near detector

M. Atkinson, P. Coloma, I. Martinez-Soler, NR, I Shoemaker, JHEP 04 (2022) 174

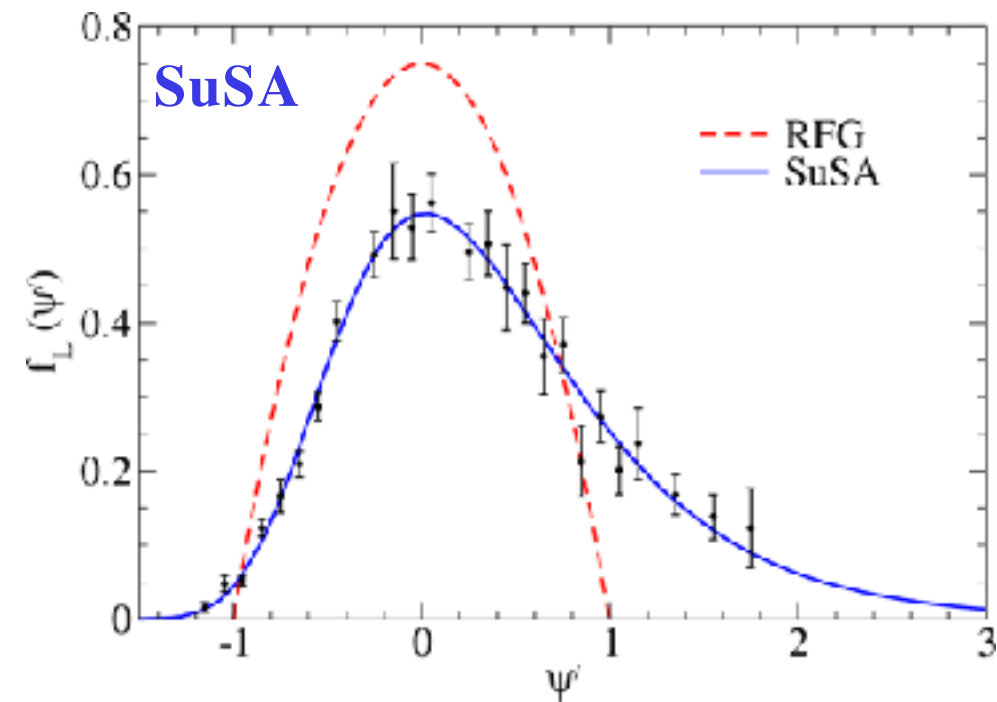
- Neutrino cross sections in the quasi elastic regime, for arbitrary Weak EFT interactions

Z. Tabrizi, J. Kopp, NR, in preparation



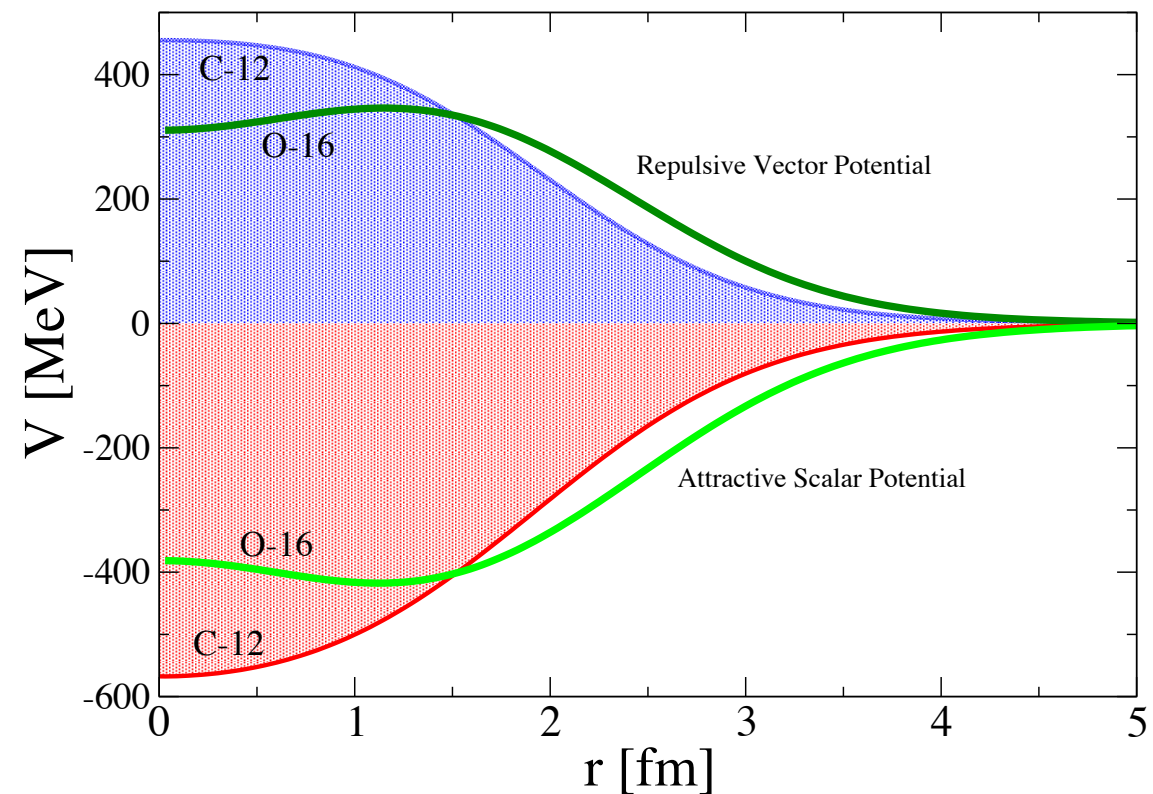
# Super-Scaling (SuSA) model

Amaro *et al.*, PRC71 (2005)



Basic idea is to use the scaling function extracted from longitudinal (e,e') data to predict  $\nu$ -scattering cross sections

Gonzalez-Jimenez *et al.*, PRC90(2014)



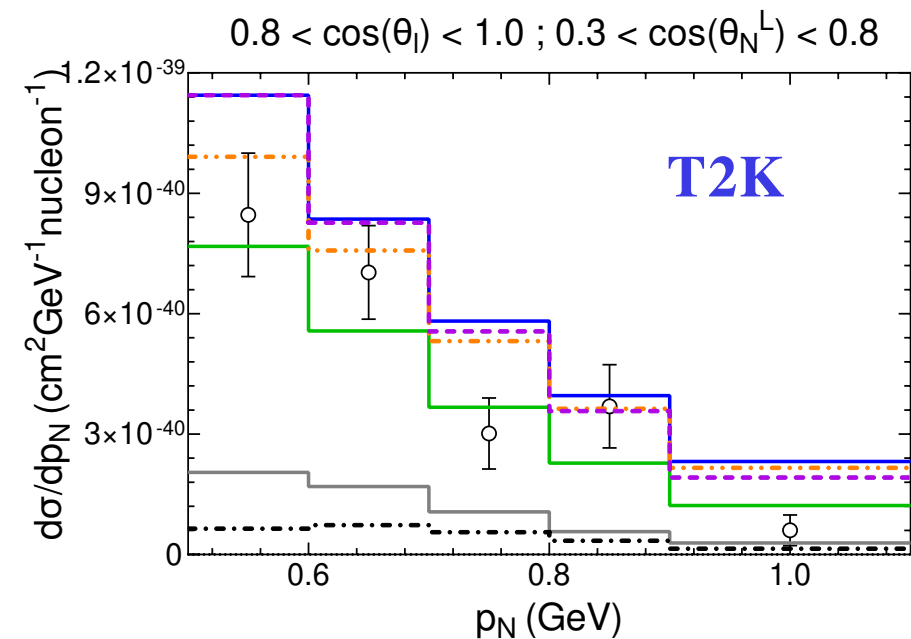
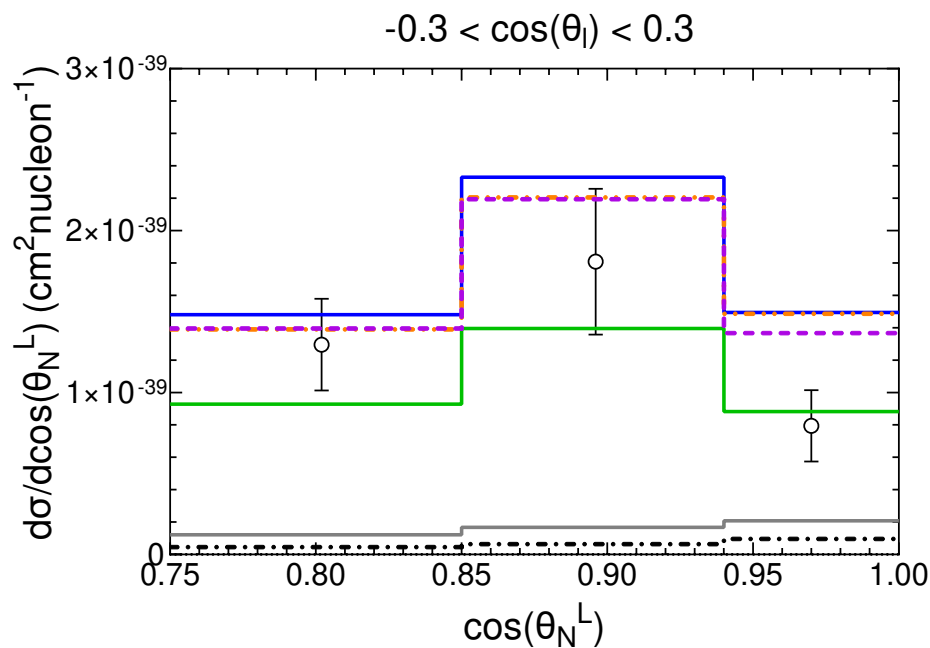
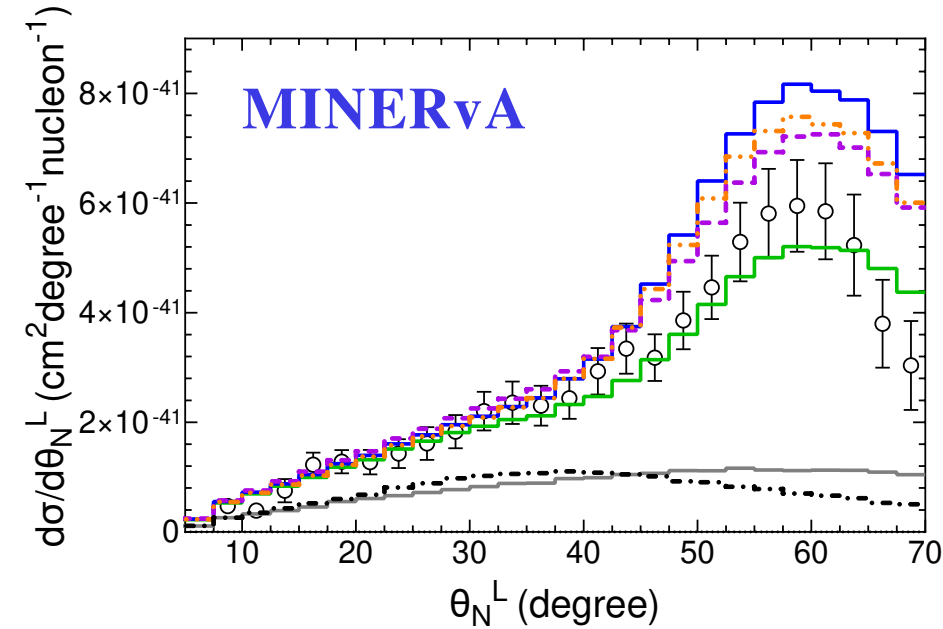
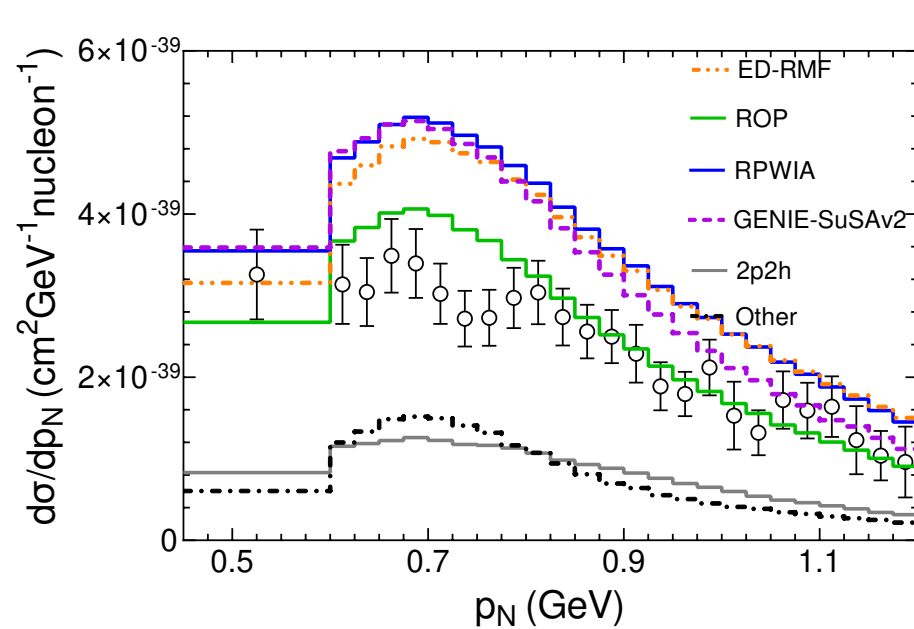
The nuclear wave functions are solutions of the Dirac equation with phenomenological relativistic scalar and vector mean field potentials

$$(i\gamma^\mu \partial_\mu - M - S + V) \psi(\vec{r}, t) = 0$$

**SuSAv2** : uses scaling functions extracted from Relativistic Mean Field calculations.

$f_T > f_L$  in agreement with L/T separated (e,e') data

CC0 $\pi$  semi-inclusive  $\nu_\mu$  -  $^{12}\text{C}$  cross section as a function of the proton kinematics



All curves include the 2p2h and pion absorption contributions evaluated using GENIE

# Conclusions

---

- \* Neutrino oscillation experiments are entering a new precision era

- \* To match these precision goals accurate predictions of neutrino cross sections are crucial

  - Ab initio methods: almost exact results but limited in energy, fully inclusive

  - Approaches based on factorization schemes are being further developed

- \* Uncertainty associated with the theory prediction of the hard interaction vertex needs to be assessed. Initial work has been carried out in this direction studying the dependence on:

  - Form factors: one- and two-body currents, resonance/ $\pi$  production

  - Error of factorizing the hard interaction vertex / using a non relativistic approach

- \* Overall, there has been great progress in the implementation of theory models in event generators but more work is still needed

- \* Combine state-of-the art neutrino-nucleus calculations with BSM theories is gaining momentum

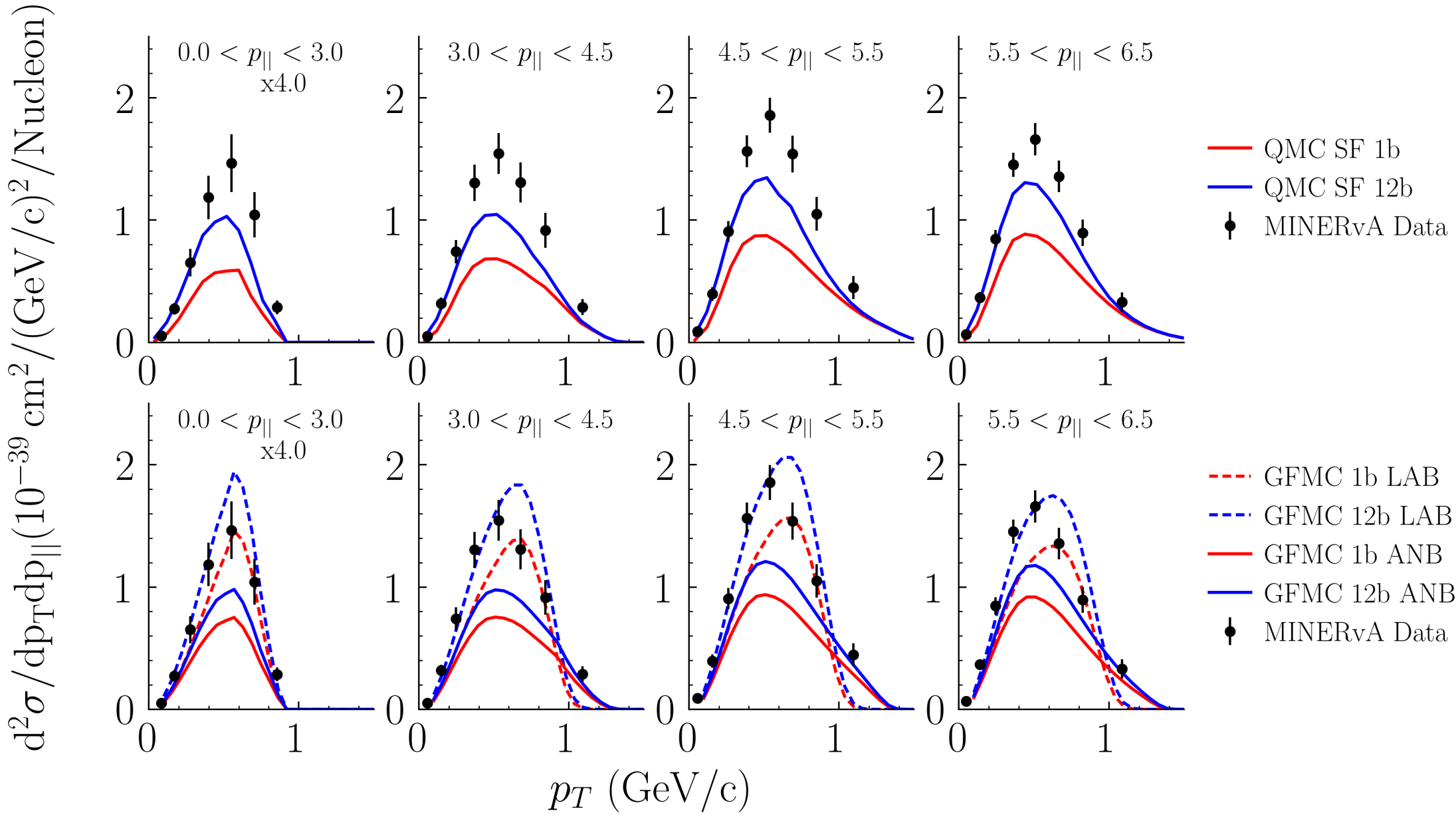
Thank you for your attention!



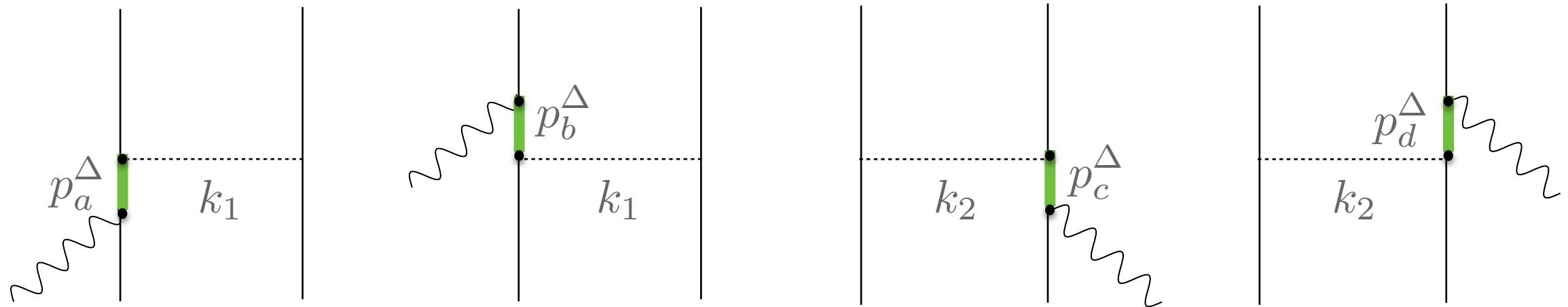
# Comparing different many-body methods

–MINERvA M.E. Double Differential Cross Section in  $p_T$ ,  $p_{||}$ . CCQE-like data on CH

N. Steinberg, A. Nikolakopoulos, A. Lovato, NR, *submitted to Universe*



# Two-body currents - Delta contribution



$$j_{\Delta}^{\mu} = \frac{3}{2} \frac{f_{\pi NN} f^{*}}{m_{\pi}^2} \left\{ \Pi(k_2)_{(2)} \left[ \left( -\frac{2}{3} \tau^{(2)} + \frac{I_V}{3} \right)_z F_{\pi NN}(k_2) F_{\pi N\Delta}(k_2) (J_a^{\mu})_{(1)} \right. \right. \\ \left. \left. - \left( \frac{2}{3} \tau^{(2)} + \frac{I_V}{3} \right)_z F_{\pi NN}(k_2) F_{\pi N\Delta}(k_2) (J_b^{\mu})_{(1)} \right] + (1 \leftrightarrow 2) \right\}$$

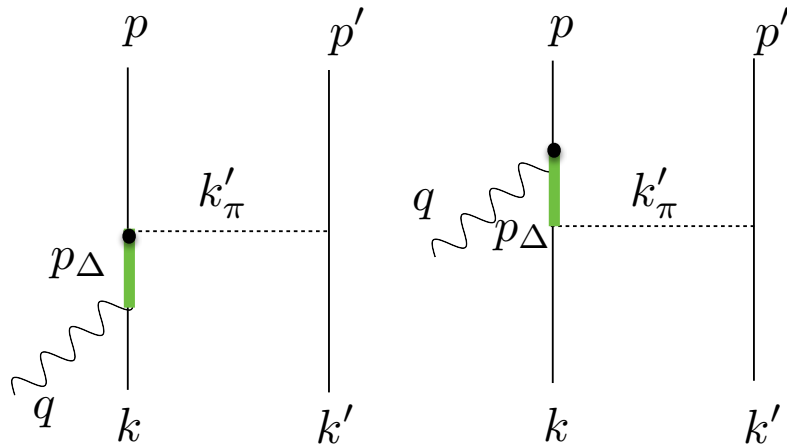
where

Rarita Schwinger propagator

$$(J_a^{\mu})_V = (k_1)^{\alpha} G_{\alpha\beta}(p_{\Delta}) \left[ \frac{C_3^V}{m_N} \left( g^{\beta\mu} \not{q} - q^{\beta} \gamma^{\mu} \right) + \frac{C_4^V}{m_N^2} \left( g^{\beta\mu} q \cdot p_{\Delta} - q^{\beta} p_{\Delta}^{\mu} \right) \right. \\ \left. + \frac{C_5^V}{m_N^2} \left( g^{\beta\mu} q \cdot k - q^{\beta} k^{\mu} + C_6^V g^{\beta\mu} \right) \right] \gamma_5$$

# Delta contribution to MEC

Diagrams including the Delta current depend on many parameters.



$$\begin{aligned}
 (j_a^\mu)_A &= (k'_\pi)^\alpha G_{\alpha\beta}(p_\Delta) \left[ \frac{C_3^A}{m_N} (g^{\beta\mu} \not{q} - q^\beta \gamma^\mu) \right. \\
 &+ \frac{C_4^A}{m_N^2} (g^{\beta\mu} q \cdot p_\Delta - q^\beta p_\Delta^\mu) \\
 &\left. + C_5^A g^{\beta\mu} + \frac{C_6^A}{m_N^2} q^\mu q^\alpha \right],
 \end{aligned}$$

Parametrization chosen for the vector ff:

$$C_5^A = \frac{1.2}{(1 - q^2/M_{A\Delta})^2} \times \frac{1}{1 - q^2/(3M_{A\Delta})^2},$$

Current extractions of  $C_5^A(0)$  rely on single pion production data from deuterium bubble chamber experiments; estimated uncertainty  $\sim 15\%$

$$\text{Delta decay width: } \Gamma(p_\Delta) = \frac{(4f_{\pi N\Delta})^2}{12\pi m_\pi^2} \frac{|\mathbf{d}|^3}{\sqrt{s}} (m_N + E_d) R(\mathbf{r}^2) \qquad R(\mathbf{r}^2) = \left( \frac{\Lambda_R^2}{\Lambda_R^2 - \mathbf{r}^2} \right)$$